SMHI RMK
No 62, 1991

A FIELD TEST OF THERMOMETER SCREENS

by

Tage Andersson and Ingemar Mattisson

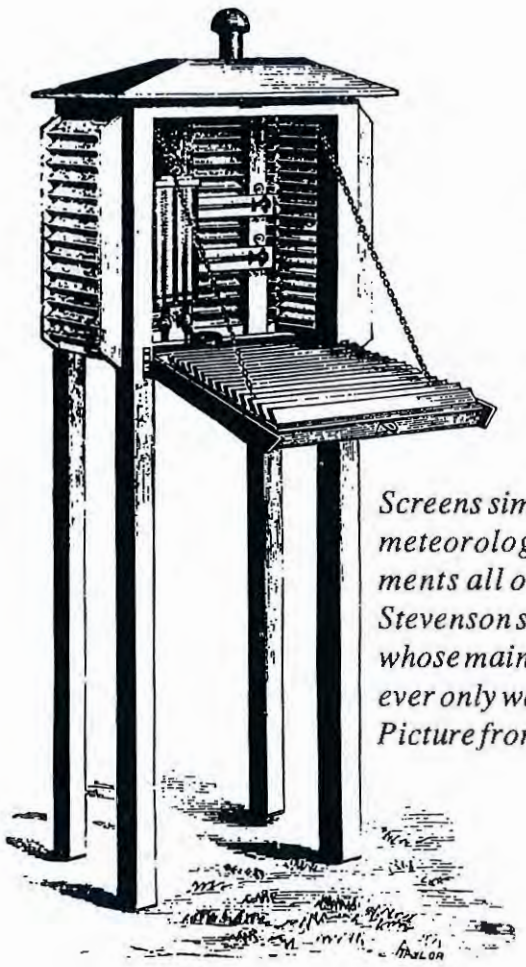

Screens similar to this one are now used for meteorological air temperature measurements all over the world. They are called Stevenson screens after Thomas Stevenson, whose main contribution to the design however only was the double louvres. Picture from 1879.

No 62, 1991

REPORTS
METEOROLOGY and CLIMATOLOGY

A FIELD TEST OF THERMOMETER SCREENS

by

Tage Andersson and Ingemar Mattisson

Printed in Sweden, SMHI Norrköping 1991

Issuing Agency

SMHI
S-601 76 Norrköping
SWEDEN

Report number

RMK 62

Report date

April 1991

Author (s)

Tage Andersson and Ingemar Mattisson

Title (and Subtitle)

A field test of thermometer screens

Abstract

For a period of nearly one year temperature readings from small sensors (high quality platinum resistance thermometers) in conventional screens (Stevensson type) and smaller screens (Lambrecht, Young and Vaisala) have been compared to those from a sensor of the same type in a ventilated screen (Teledyne). The test was financially supported by the Swedish Civil Board of Aviation and CDS Mätteknik, Skara. The reading from the Teledyne screen was used as reference and considered the 'true' air temperature. The deviations from the reference were mainly due to two factors:

- the thermal inertia of the screens
- radiation errors.

The thermal inertia is largest for the larger screens. With rapid air temperature changes and calm winds the larger (Stevenson) screens lag behind much more than the smaller ones. Also the radiation errors are largest for calm winds. The extreme errors then occur during calm winds and clear sky. The errors found are larger than given in the literature. The largest error noted, +3.6°C for one of the Stevenson screens, occurred a calm, clear evening. Generally the extreme errors occurred at sunset and sunrise, not in the afternoon when the irradiation has its maximum, because it then usually is windy. Generally the smaller screens followed the reference better than the Stevenson ones. However, with calm winds, clear sky and snow cover the small screens may rapidly get overheated. The averages for longer periods (months) generally differed less than 0.1°C from the reference. In fact, the formulas used for computing climatological mean temperatures when only few regular measurements are available gave larger differences than the screens.

Key words

Temperature measurement techniques
Thermometer screens

Supplementary notes

Number of pages

41

Language

English

ISSN and title

0347-2116 SMHI Reports Meteorology and Climatology

Report available from:

Swedish Meteorological and Hydrological Institute (SMHI)

A FIELD TEST OF THERMOMETER SCREENS

by

Tage Andersson and Ingemar Mattisson
Swedish Meteorological and Hydrological Institute (SMHI)

1. Introduction

For small temperature sensors used in automatic data acquisition systems the old conventional screens, capable of housing several liquid thermometers and even a recording bimetallic thermograph are unnecessarily large. Since those old screens are also rather expensive to manufacture and maintain it is natural to look for smaller and more cost-effective altematives. A very small number of such screens are already used in Sweden in meteorological networks for special purposes, at airports and at stations in the official network of synoptic and climatological stations. Since a change of thermometer screen may affect single observations as well as temperature records a comparision between the conventional, wooden screens and the new ones was needed. For these reasons a field test has been performed. The work reported here has partly been financed by the Swedish Civil Aviation Board.

Two types of wooden screens (Stevenson type) are now used in Sweden. Our test included those and 3 types of commercially available smaller screens. All these screens are unventilated. To get as good an estimate as possible of the air temperature a ventilated screen was used to produce a reference temperature. (In an unventilated screen the air passes through the shield driven by the wind only, while in a ventilated screen the air is sucked through the shield by a motordriven fan.)

Since the wooden screens used in the official network sometimes may be less well maintained (the importance of keeping a clean, white surface is always stressed in instructions and also considered necessary) a screen in rather bad condition was included. Of the three types of smaller screens one is used at some airports and also by the road authorities. The latter ones have a special mounting, on a short arm at the side of a long pole instead of a short arm at the top of a short pole. Those screens, complete with mountings, were therefore included. Altogether the experiment thus comprised seven unventilated and one ventilated screen. Besides there were auxiliary sensors giving wind speed and direction, relative humidity, net radiation and precipitation (yes/no), all at the same level above the ground (1.5 m). Data were automatically stored at one-minute intervals.

Radiation data from the radiation measuring station of SMHI were also used. The sensors were situated at a roof about 200 m east of the screens.

Hourly synoptic observations were available from Bråvalla 4 km northwest of the test site. Quantitative precipitation recordings were furnished by two tipping bucket precipitation gauges (recorded on drums). The litterature on the error sources of ordinary screens is so extensive that it might seem unnecessary to include the SMHI screens in an investigation of this type. However, most investigations are old, performed with oldtechniques and with screens not available today. We have not tried to study all older works, but mainly used a summary by Sparks (1972).

2. Experimental setup

The experiment was performed at the SMHI observation test site in Norrköping, a fairly unobstructed grass surface. The site is not quite plain but forms a weak depression and there are some close obstructions as small huts and masts for meteorological observations and some other instruments, see Fig 1. Fig 2 shows the arrangement of the instruments.

As temperature sensors were used platinum resistance thermometers of type PT 100, 0.1 DIN 43760. Before and after the test the quality of the sensors was controlled by calibration at SMHI. The first two deliveries were rejected due to non-compliance with the DIN specification.

The sensors were connected to a HP scanner and HP digital multimeter. A HP clock gave time and day. Scanner, multimeter and clock were controlled by a PC/AT via a GPIB bus. The PC/AT stored data on a hard disc. The overall accuracy of the temperature measurements was estimated to ±0.04°C.

An overview of sensors and screens is given in Table 1.

Table 1. Sensors and screens used

T0	Constant reference precision resistance, 100 Ohm, placed in a junction box.
T1	Teledyne screen type 327B, ventilated, 10 feet/s. Used as reference.
T2	Lambrecht screen, catalogue no 814, aluminium, eloxal processed, diameter 17 cm, height 44 cm, on short pole.
T3	Lambrecht screen, catalogue no 814, aluminium, eloxal processed, diameter 17 cm, height 44 cm, on long pole.
T4	Young screen, model 4104, white thermoplastic, diameter 12 cm, height 27 cm.
T5	SMHI screen, large, wooden, in good condition, width*depth*height = 70*53*81 cm.
T6	SMHI screen, large, wooden, in rather bad condition, 70*53*81 cm.
T7	SMHI screen, small, wooden, in good condition, 40*40*68 cm.
T8	Vaisala screen, type DTR11, fiber glass reinforced polyester, diameter 22 cm, height 29 cm.
VH	Wind speed, Teledyne 1564B, interface 20.11/2012 .
VR	Wind direction, Lambrecht 1466/E7.
RH	Relative humidity, Lambrecht 800L100.
NR	Net radiation, Siemen Ersking.
NB	Precipitation, Vaisala DPD 12A (Yes/No).

We can note that all screens, except the Lambrecht, have a white outer surface. A more detailed description is given in Appendix 1.

All data were measured 12 times per minute. Arithmetic one minute averages were recorded for all except for wind direction and precipitation, where momentary values were recorded once every minute. (One minute averages for surface observations of air temperature for synoptic purposes is recommended by WMO, 1983).

The test period was April 1989 through February 1990.

3. Statistical parameters used

The reference screen, Teledyne, is considered to give the true air temperature. Our main parameter will be the difference from this one, i e

DIFF(screen) = T(screen) - T(ref)

T(screen) = Temperature according to screen, °C

T(ref) = Temperature according to sensor in the Teledyne screen.

For each day with complete observations the following statistics have been computed:

Number of observations	N (=1440)
Arithmetic mean	$MV(screen) = \Sigma\ DIFF(screen)/N$
Root mean square	$RS(screen) = \sqrt{\Sigma\ DIFF(screen)^2/N}$
Cube mean square	$SKEWN(screen) = \sqrt[3]{\Sigma\ DIFF(screen)^3/N}$
Max of Diff(screen)	MAX(screen)
Min of DIFF(screen)	MIN(screen)

These statistics have been computed for single days with complete records as well as for longer periods.

3.1 Overview of the results

In order to introduce the main results Table 2 gives statistics for 207 days with complete records.

Table 2a shows that the average of DIFF, MV, is of the same order of magnitude as the overall accuracy of the measuring system. From this quantity then nothing can be said about any possible differences between the screens. The root mean square, RS, is smallest for the Vaisala and Young screens (Nos 8 and 4 resp). Of the SMHI screens the one in bad condition (6) has the largest RS value, verifying the old rule that a screen shall be kept in good condition with a clean, white surface. The difference in scatter is very large, that of the SMHI screen in bad condition being nearly twice that of the Vaisala. The mounting of one Lambrecht on a long pole (No 3) instead of on a short one did not affect the measurements very much. The long pole however got somewhat larger RS than the short one and also the skewness was somewhat larger, indictating a small effect of the pole.

A positive value of the SKEWN means that the frequency distribution has a longer tail towards the positive side. All screens except the Vaisala have positive skewness. As to the extreme values mainly the same applies as to RS, i e the Vaisala has the smallest (absolute) extremes and the SMHI screens the largest, the screen in bad condition being worst.

Table 2. Statistics for April 1989 - February 1990

The following notations have been used:

For parameters

DIFF = arithmetic difference from the reference temperature, i.e. (temp(shield)-reference temp), in °C.

The following statistics have been prepared for each day:

MV = average of the diff
RS = root mean square of the diff
SKEWN = cube mean square of the diff
MAX = maximum of the diff
MIN = minimum of the diff

For screens

8 = Vaisala screen
7 = small SMHI screen
6 = ordinary SMHI screen in rahter bad condition
5 = ordinary SMHI screen in good condition
4 = Young screen
3 = Lambrecht screen, on long pole
2 = Lambrecht screen, on ordinary pole

Table 2a. Average values

SCREEN	MV	RS	SKEWN	MAX	MIN
8	-0.01	0.154	-0.12	0.47	-0.41
7	0.04	0.227	0.26	0.83	-0.56
6	0.01	0.295	0.32	1.00	-0.75
5	0.00	0.241	0.26	0.87	-0.62
4	0.00	0.168	0.17	0.56	-0.50
3	0.04	0.215	0.24	0.59	-0.46
2	0.01	0.209	0.17	0.55	-0.51

Table 2b. Extreme values of diff

SCREEN	MAX	MIN
8	2.08	-1.58
7	2.62	-1.66
6	3.61	-2.06
5	3.10	-1.68
4	3.36	-1.86
3	2.51	-1.70
2	2.49	-1.95

The deviations in Table 2b are very large compared to what is given in the literature. For instance, the WMO Guide to Meteorological Instruments and Methods of Observation (1983) says that "the temperature of the air in a screen can be expected to be higher than the true air temperature on a day of strong sunshine and calm wind, and slightly lower on a clear, calm night, with errors perhaps reaching +2.5°C and -0.5°C respectively in extreme cases". According to the standard work 'Meteorological Instruments' (Middleton and Spilhaus, 1960) the Stevenson screen may give readings more than 1°F (about 0.5°C) too high in calm, clear afternoons and a little too low in calm, clear nights.

Large (absolute) DIFFs are by far most common during summer, but also during the colder seasons the screen temperature can deviate more than 2°C from the air temperature, see Table 3 and 4.

Table 3. Statistics for June 1989. *Notations as in Table 2.*

Average values

SCREEN	MV	RS	SKEWN	MAX	MIN
8	-0.07	0.183	-0.17	0.61	-0.58
7	0.08	0.296	0.36	1.22	-0.71
6	0.08	0.375	0.45	1.46	-0.96
5	0.02	0.301	0.36	1.23	-0.80
4	-0.01	0.195	0.17	0.79	-0.68
3	0.08	0.269	0.29	0.86	-0.62
2	0.05	0.265	0.21	0.80	-0.70

Extreme values of diff

SCREEN	MAX	MIN
8	1.37	-1.58
7	2.58	-1.66
6	3.22	-2.06
5	2.67	-1.51
4	2.18	-1.34
3	2.38	-1.70
2	2.28	-1.95

Table 4. Statistics for December 1989. *Notations as in Table 2.*

Averages valaues

SCREEN	MV	RS	SKEWN	MAX	MIN
8	0.05	0.131	0.17	0.41	-0.19
7	0.03	0.181	0.21	0.61	-0.37
6	-0.01	0.249	0.27	0.75	-0.54
5	0.01	0.188	0.24	0.64	-0.40
4	0.02	0.128	0.17	0.42	-0.29
3	0.01	0.143	0.22	0.37	-0.27
2	-0.01	0.143	0.19	0.30	-0.29

Extreme values of diff

SCREEN	MAX	MIN
8	1.20	-0.41
7	1.99	-1.36
6	2.87	-1.90
5	2.22	-1.21
4	1.70	-1.14
3	2.13	-0.96
2	1.91	-0.96

During summer large positive values of the DIFFs cluster around the time of sunset (not about the time of maximum temperature) and, to a lesser degree, the early morning, while the large negative ones are most common after sunrise. Fig 3 gives the time and magnitude of the most extreme DIFFs irrespective of screen, under the conditions that this DIFF was >=2.0 or <=-1.5°C. Mostly screen nr 6 (the SMHI screen in bad condition) is represented.

To illustrate the duration of large DIFFs we defined an extended, large DIFF period as one where DIFF>=1°C lasted at least 1 hour. The numbers of such events are given in Table 5.

Table 5. Numbers of periods with DIFF > = 1°C during at least 1 hr.

Screen	No	Comments
8	0	
7	9	In May-Aug, between 18 and 22 UTC
6	14	13 in May-Aug, between 18 and 22. 1 in Dec, 12-14 UTC.
5	8	In May-Aug, between 18 and 22.
4	0	
3	5	4 in May-Aug, between 05 and 10 UTC, 1 in Dec 10-11 UTC.
2	3	In May-Aug, between 06 and 10 UTC.

Characteristic for the SMHI screens (Nos 5-7) was thus that long-lasting overheating was most common around the time of sunset, while for the Lambrechts the preferred times were after sunrise.

The corresponding statistics for negative DIFF is not so easy to produce, since the DIFF generally fluctuated considerably when negative. The extreme negative DIFF moreover generally was of less magnitude than the corresponding positive ones. However, it is quite clear that long periods with negative DIFF (average values less than about 0.5°C) almost exclusively occurred during night. They were also most common for the Lambrecht screens.

3.2 Performance of the screens in characteristic weather types

To demonstrate the performance of the screens we will show the daily march of the differences (DIFF(screen)) during some weather types.

3.2.1 Cloudy weather with and without light precipitation

Overcast, with light precipitation, varying wind speeds and only small and slow changes of the air temperature is illustrated by June 4th, 1989, Fig 4a-b. Overcast is favourable for all screens, and the DIFFs are small with RS below 0.1°C.

Cloudy with low wind speeds and insignificant solar irradiance is shown by Fig 5a-c. (The direct beam irradiance is that portion of radiant energy received at the instrument 'direct' from the sun). Despite these rather favorable conditions the DIFFs are considerable for the SMHI screens (Nos 5-7). Their natural ventilation becomes insufficient with the low winds, and they have a slow response to air temperature changes. Note especially their response to the short temperature maximum about 14:00 hr. The average temperatures for the day differ however less than 0.1°C from the reference. The explanation is that rapid temperature rises are as common as rapid drops and these errors cancel each other in the averaging. The RS however are much larger than in the preceding example, about 0.3°C for the SMHI screens and about 0.1°C for the novel ones.

The SMHI screens have a much larger mass, and probably also a less efficient natural ventilation than the novel ones. The response of the SMHI screens should then be slower.

3.2.2 Clear weather

Clear, calm winds, large air temperature amplitude and fast air temperature changes is illustrated by May 22, 1989, Fig 6a-c. These are unfavourable conditions and the DIFFS fluctuate wildly. There are pronounced differences between the screens, the Vaisala having a RS of 0.2°C, the Young 0.4°C, the Lambrechts nearly 0.6°, with the long pole mounting worst. Within the SMHI group there are also differences; the screen in bad condition being worst (0.6°) and the small one best (0.4°).

Fig 6b shows that the large screens produce a smoother curve, which is explained by their longer response time.

Note that the extremes of the DIFFs tend to occur about sunrise and sunset, NOT at the times of the temperature extremes. The screen surplus temperature is not largest at the time of maximum irradiation. The main reason for this, which is characteristic for summer days, is that during the day the wind is strong enough to ventilate the screens and prevent large deviations from the air temperature, Fig 6c. At sunrise and sunset the wind often is much lower. The extreme positive DIFFs for the SMHI screens (about 2°C) occur at the rapid cooling after sunset, with calm winds. It is interesting that the extreme positive DIFFs for the Lambrecht (also about 2°C) instead occur about 3 hr after sunrise, when it still is calm. The Lambrecht screen evidently offers somewhat less efficient radiation shield. This day they generally gave a temperature surplus of 0.5°C or more from 05:00 to 16:00 hr. With the exception of the Lambrechts the day's average temperatures only differed a few hundreds of a degree from the reference.

Another example of a clear day with low wind speed, July 26, Fig 7a-c, shows a quite different pattern. During 00:00-03:00 UTC only the Lambrecht (Nos 2,3) screens show sligthly negative DIFFs, and some screens even show POSITIVE ones.The early night hours of May 22, Fig 6a and b, were calm and all screens had negative DIFFs. According to Fig 7b then a wind speed of only about 0.5 m/s (at the 2 m level) gives sufficient natural ventilation during the night to prevent radiation losses. Some night-time fluctuations of the DIFFs (Fig 7a) are conspicuously large for the SMHI screens. Those occur at rapid air temperature changes and can, as in the preceding examples, be explained by a long response time of the screen.

During day-time July 26 had only slightly higher wind speeds than May 22, but nevertheless much smaller positive DIFFs. Thus the wind speed is very important, and there are probably values where the ventilation becomes efficient enough to prevent large (absolute) DIFFs. If not taken too literally these values may be called thresholds in the sense that with wind decreasing below them the radiation error increases rapidly, cf Appendix 1, description of the Young screen. The thresholds evidently depend upon the screen type. Thus we should NOT expect one single threshold. Another noteworthy feature of July 26 is that during day-time the Vaisala screen (No 8) has NEGATIVE DIFFs. This has repeated itself several days and is hard to explain. Fig 7c displays a very regular march of the net radiation. Comparing with Fig 7a it is evident that the extreme DIFFs do not occur at the times of maximum irradiation.

Varying cloudiness is accompanied by rapid air temperature changes, and very varying DIFF, especially for the SMHI screens, see Aug 30, Fig 8a-b. Not also here the large surplus of the SMHI screen No 6 after sunset.

3.2.3 Clear with snow cover

Large absolute DIFF occur also in clear weather during winter, in spite of the low solar elevation (below 9°), see Fig 9a-c, Dec 13. This was a sunny day, nearly 6 hours of sunshine, with low winds and a snow cover. Most of the significant DIFFs here are connected to rapid air temperature changes, and therefore are explained by the differing response times. The Lambrechts, Nos 2 and 3 in Fig 9a, however also shows another feature,a long-lasting temperature surplus during the sunshine hours, in spite of the low sun elevation and a wind speed of about 1 m/s.

After a light snowfall 00:00-06:00 hr Nov 28 the sky broke up, the wind decreased and a day with fresh, clean snow cover gave us interesting results, see Fig 10a-c. The Lambrechts reacted immediately to the irradiation with a temperature surplus of about 1°C between 10:30 and 13:30, despite a wind speed of about 1 m/s at 10:30. At a lull just after 12:00 hr the DIFFs reached 2.5°C for the screen on the long pole (No 6). At the same time also the Young reached a DIFF of 2°C during a short peak. But until 12:00 hr the Young, as well as the SMHI and Vaisala screens, resisted the irradiation. Then the DIFF of the SMHI screens began to rise, and when the air temperature rapidly dropped (about 4°C between 13:00 and 14:00 hr) the DIFFs reached a peak (2°C for screen No 6, 1.6°C and 1.5°C for Nos 5 and 7 respectively). With a smaller irradiance the weak wind however did ventilate the Lambrechts enough to reduce the surplus temperature considerably.

We may be pretty sure that these temperature surplus of the Lambrechts are caused by reflected (diffuse or direct) sunshine from the snow cover. On a day with similar weather but no snow cover, Nov 17, Fig 11, the Lambrecht with ordinary mounting (No 2) only showed a small surplus.

We must, however, not conclude that the other screens are free from this snow cover radiation error. Fig 12, Dec 16, another sunny winter day with calm winds, shows that the other screens recorded too high temperaturesalso when the air temperature remained nearly constant, see 09:00 to 12:00 hr that day. The overheating of the Lambrechts started about 1 hr earlier than forthe other screens, but also they reached considerable DIFFs, about 1°C for the SMHI and Vaisala, nearly 2°C for the Young (the Lambrechts about 2°C). In the rapid temperature drop between 13:00 and 14:00 (5°C) the SMHI screens reached DIFFs of 2°C or more.

Aluminium color absorbs more shortwave radiation than white (Middleton, 1960, Fuchs and Tanner, 1965) and also the black color on the down-facing surface of the lowest annulus of the Lambrecht screen may contribute to the overheating.

We can thus conclude that a snow cover may cause considerable radiation errors. This error should increase with the solar elevation. Unfortunately our record does not include any days with higher solar elevation and snow cover, but this radiation error must then be expected to be large, not only for the Lambrecht screen. The problem is that this weather type is fairly common in northern and middle Sweden during late winter and spring.

3.2.4 Fog and rain

An interesting day with several weather types is Nov 3, Fig 13a-c. This day started with fog, sky clear according to the observation at Bråvalla. At 02 UTC the fog had thickened and the sky was obscured. Between 02:40 and 05:10 drizzle was reported, with visibility below 500 m. During the day there was no precipitation, but moderate rain between 17:25 and 21:30 (accumulated precipitation 9 mm).

During the calm winds of the first hour of the day the temperature fluctuated, and so did the DIFFs. The fluctuating temperature indicates a ground inversion. The rapid temperature rise, about 0.7°C/minute just after 01:00 hr occurred when the wind was increasing and the net radiation rising, Fig 14. The ground inversion was dissipated and the smooth temperature curve after the rise indicates an adiabatic lapse rate. Probably the fog thickened just at the time of the temperature rise. During the temperature rise the DIFFs were negative for the SMHI screens, but positive for the novel ones. Thus the novel screens reacted FASTER than the reference, while the opposite is true for the SMHI ones. This indicates that the natural ventilation of the novel screens then was more efficient than the artificial of the reference one. During the moderate rain (between about 17:30 and 21:30 hr) the temperature was steady and the DIFFs were very close to zero.

3.2.5 Showers

June 28, Fig 15a-c, illustrates the effects of showers. The first half of that day several small showers do not show up in the DIFFs. A heavy shower at 13 UTC with rain rates up to about 1 mm/min was accompanied by a cooling of about 5°C during 10 minutes. The response of the Lambrecht, Vaisala and Young screens was FASTER than that of the reference, while the opposite is true for the SMHI screens, Fig 16. Thus the DIFFs for the SMHI screens were positive during the cooling, while the DIFFs for the others were negative, see Fig 15a . This behaviour, i. e. negative DIFFs for the novel screens and positive for the SMHI, is analogous to that observed during the rapid temperature rise Nov 3. The most natural explanation is thus that the considerable DIFFs observed during this and some other showers are not caused by evaporational cooling or any other cooling of the screens by the rain, but the rapid cooling, which in its turn may be dependent upon the rain intensity. During those conditions the differences between screen temperatures may become very large. For instance at 13:14 hr June 28 screen No 2 (Lambrecht) gave 16.2°C and screen No 6 (SMHI, bad condition) 19.4°C, a difference of 3.2°C in overcast with moderate wind speed!!

Evaporational cooling should give too low screen temperatures after showers. After the main shower of Jun 28 the relative humidity dropped from about 95% to about 90%, Fig 15b. Small negative DIFFs then observed at the SMHI gauges no 5 and 6 are explained by a rapid air temperature rise. We have not observed any evaporational cooling, which however may be due to the rareness of heavy showers in our climate.

3.2.6 Snowfall

An example of moderate snowfall with temperatures close to 0°C on Dec 12 is given by Fig 17. The DIFFs are very close to 0 as should be expected. Falling snow can accumulate on the screens and adversely affect the ventilation. Wet snow may stick to them, forming a large mass and destroying the ventilation. In the worst case the snow may freeze and remain for a long period. The winter of 1989-1990 was however unusually mild and we have few examples of snowfall.

3.2.7 Discussion

The examples discussed and inspection of numerous other graphs reveal that a rapidly varying air temperature is the main cause for large fluctuations in the DIFFs. Compared to the novel screens the SMHI ones have a large mass, double louvers and a small ratio (total surface area)/volume. The large mass contributes to a long response time. The double louvres and small surface area/volume ratio certainly give a less efficient natural ventilation. Also the influence of radiation changes should be least for a large screen with small surface/volume ratio. The net result is a longer response time and large fluctuations of the DIFFs for the SMHI screens. So different response times are the main cause for the short-time fluctuations of the DIFFs.

More long-lived, but generally smaller absolute DIFFs are caused by radiation errors. The Lambrechts seem to offer somewhat less efficient radiation shielding than the other novel screens tested.

The largest scatter occurs with low cloudiness and calm or very light winds at sunrise and sunset, when the air temperature is rapidly changing, Figs 6 and 7.

The behaviour is quite complex, see Figs 18 and 19. Just after sunrise, when the air temperature starts rising, the screens lag behind and give negative DIFFs. The SMHI screens are worst in this respect, DIFFs often reaching below -1°. The probable reason is bad natural ventilation. After about two hours there are large positive DIFFs, probably caused by radiation heating. Worst in this respect are the Lambrecht and Young screens, DIFFs often reaching above 1°. The DIFFs decrease when the wind speed increases.

At sunset, when the wind decreases and the temperature rapidly drops, the screens give positive DIFFs. The process is heavily dependent upon the wind speed. It often starts about 2 hours before sunset and is caused by less efficient natural ventilation when the wind decreases. The by far largest DIFFs occur for the SMHI screens, often above2°. The maximum DIFF noted was 3.6°C for the SMHI screen in bad condition. This occurred about half an hour before sunset, July 2. At the same occasion the Young screen had a DIFF of 3.4°, but the Lambrecht ones only 1.7° and 1.6° respectively.

Already in 1913 Köppen described an afternoon overheating of about 1°C in summer afternoons with clear skies in middle and northern Europe (Stevenson screen). That we have found much larger errors is natural since Köppen's data were confined to some fixed times and the extremes may have eluded him. Moreover the maximum surplus temperatures occur much later than Köppen anticipitated. Generally they do not occur at the time of maximum irradiation (from the sun or ground) but when this is fairly low. Their main cause is a combination of rapid air temperature change and bad natural ventilation of the screens. Thus the commonly used term 'radiation error' is misleading.

With calm winds, clear and only small rapid air temperature fluctuations the DIFFs fluctuated strongly, but their magnitude was generally only about 0.5°C. That is, during clear calm nights the screen temperatures averaged about 0.5°C below the air temperature and during nearly calm, clear days about 0.5°C above. There was never absolute calm on the middle of clear summer days, i. e. when the irradiation had its maximum. There is some variation between the screens. The Vaisala generally was closest to the reference, while during calm winds of clear summer days the Lambrechts tended to show the largest DIFFs. This is probably due to the aluminium color of these screens. That color leads to greater errors in sunshine (Middleton and Spilhaus,1960). As mentioned earlier extremes of DIFFs needed a rapid air temperature change of some degrees. Those temperature changes are most common near sunrise and sunset, and therefore the extreme DIFFs tend to occur at those times. Also at those occasions the Vaisala screen generally agreed best with the reference.

Thus there must be an annual march of the DIFFs. The behaviour at sunrise and sunset is however much influenced by shadows from nearby objects. Those are most frequent with low solar elevation angles. In a network of stations therefore each station will have its own annual march, depending on the surrounding shadow-casting objects.

During clear days with snow cover the irradiation is greatly enhanced, and with calm winds large radiation errors must be expected.

4. Effects of screen condition and mounting

As mentioned in the introduction, one of the SMHI screens was in rather bad condition, and one of the Lambrechts had a special mounting on a long pole.

The SMHI screen mentioned was not in really bad condition. The painting was old, some paint had flaked off, but otherwise no differences between this one and the one in good condition could be detected at visual inspection. It is certainly possible to find worse screens in the official network. Nevertheless, this screen (No 6) had longer response time than the one in good condition (No 5). Nearly always the screen in bad condition showed the most extreme DIFFs, which is evident from Tables 2-5. We find this clear deviation somewhat amazing. In this connection it must be noted that screens close to roads very soon become dusty and dirty, which adversely affects their ability to reflect sunshine.

The Lambrecht on the long pole (No 3) was not mounted just at the pole, but on a short horizontal arm. A small effect of the pole is perceptible in the statistics, Table 2a, where both the root and cube mean squares are somewhat larger than for the screen with ordinary mounting (No 2). Most probably the differences are due to radiation heating from the pole. Inspection of the graphs shows that on clear days and days with varying cloudiness the screen on the pole tended to give somewhat higher readings (order of magnitude 0.1°C), while during nights and overcast days no differences could be found.

5. Effects of screens and computational methods on some temperature statistics often used in climatology

Of special climatological interest are some temperature statistics. First of these is the average temperature for longer periods, as months. According to Tables 2-4 the differences caused by the screens (MV) have a magnitude less than 0.1°C, or only about our measuring accuracy.

There are also other climatologically interesting temperature statistics, such as the average temperature of a day, and the day's maximum and minimum temperature. Table 6 a-c gives average (MV), root mean square (RS) and extreme values of these quantities' differences from those according to the reference screen. As to the average temperature of single days, Table 6a, the RS is less than 0.1°C and the extreme difference noted only 0.3°C.

As to the maximum and minimum temperatures of the day, Tables 6 b-c, the RS are much larger, about 0.25°C, as well as the extreme values, which may reach somewhat above 1°C. Those differences have however much smaller magnitude than the extremes of Tables 2-4, again showing that the extreme differences generally do not appear at the times of maximum or minimum temperature.

Table 6. Differnces between screens.

Table 6a. Differences from the reference screen. Arithmetic average temperature of the day.

	MV	RS	MAX	MIN
8	-0.01	0.066	0.25	-0.17
7	0.04	0.067	0.25	-0.10
6	0.01	0.068	0.21	-0.12
5	0.00	0.051	0.16	-0.15
4	0.00	0.050	0.18	-0.13
3	0.04	0.075	0.30	-0.12
2	0.01	0.061	0.23	-0.15

Table 6b. Differences from the reference screen. Maximum temperature of the day.

	MV	RS	MAX	MIN
8	-0.11	0.215	0.37	-0.81
7	-0.07	0.213	0.78	-1.00
6	-0.12	0.242	0.45	-1.25
5	-0.15	0.263	0.42	-1.10
4	0.00	0.179	1.05	-0.71
3	0.20	0.304	1.12	-0.47
2	0.18	0.304	1.34	-0.33

Table 6 c. Differences from the reference screen. Minimum temperature of the day.

	MV	RS	MAX	MIN
8	0.10	0.151	0.51	-0.16
7	0.18	0.278	0.95	-0.57
6	0.19	0.322	1.07	-0.90
5	0.21	0.311	1.06	-0.59
4	0.00	0.142	0.36	-0.48
3	-0.08	0.164	0.33	-0.55
2	-0.13	0.208	0.31	-0.70

Climatological stations generally make observations only at some fixed times (06, 12 and 18 UTC) and have special thermometers giving the maximum and minimum temperatures of the day. To get the average temperature of the day (or month etc) from such observations there are several formulas. In Sweden the Ekholm-Moden formulas (Moden, 1939) are used:

$$tm = p*t06 + q*t12 + r*t18 + s*tmin + t*tmax$$

tm = average temperature of the day
t06, t12, t18 = temperature at 06, 12 and 18 UTC respectively
tmin, tmax = minimum and maximum temperature of the day
p, q, r, s, t = coefficients, depending upon the month and longitude. (p+q+r+s+t=1.0).

A simpler formula recommended by the WMO (1989) is

$$tm = (tmax + tmin)/2$$

To estimate the error caused by use of these formulas we have for each day with complete records computed the average temperature for the reference screen

1 as the arithmetic mean of the 1440 observations
2 according to the Ekholm-Moden formula
3 as (tmax+tmin)/2

Table 7 gives the differences from (1) in the same way as Table 6.

Table 7. Daily average temperatures according to 3 different formulas.

1: Arithmetic mean of the 1440 readings for each day.
2. Ekholm-Modens formulas
3: (max+min)/2
The table gives the differnces from (1).

	MV	RS	MAX	MIN
2	0.01	0.369	1.29	-0.93
3	-0.37	0.813	1.56	-2.81

The Ekholm-Moden formula gives a very small average difference (MV).Remembering that the RS originates from about 200 observations, the standard error of the average can be estimated as

$$\sqrt{0.369^2-0.01^2}/\sqrt{200} = 0.026$$

and the average is thus not significantly different from 0 .

The formula tm=(tmax+tmin)/2 gives a mean difference of -0.37°C. It is known that this formula usually gives a negative error, since the temperature curve is generally peaked at the minimum, while it is a broad plateau at the maximum. The standard error of the mean is 0.048 and the mean is thus significantly different from 0 (on a very high level of significance).

Comparing the RS of Table 7 with those of Table 6 it is evident that the formulas cause larger errors than the screens.

6. Conclusions

Though the measurements were performed during eleven months, the winter and spring conditions are underrepresented. This must be borne in mind when reading our conclusions.

In spite of the large absolute errors of individual screen temperatures observed (in extreme cases about 3°C), the average differences from the reference for longer periods such as months were of the same magnitude as the measurement accuracy. This applies to all the screens tested. Mostly, large absolute values of the differences are caused by the varying response times, and those errors cancel each other. The radiation errors are both positive and negative and also tend to cancel each other. One difficult condition for unventilated screens, calm, clear weather with snow cover and higher solar elevation, did not occur during the test. With reservation for that, and that winter conditions are underrepresented, introduction of a novel screen of the types tested should not be expected to cause a break in the climatological records. The root mean square error for individual observations was about 0.2°C.

Due to varying response times the screens reacted differently to air temperature changes. The large wooden screens responded most slowly, and therefore as a rule deviated most from the reference temperature. The screens divided themselves into two groups:

* the large, wooden screens of the SMHI type
* the smaller, novel screens

We can further conclude that:

* The novel screens mostly followed the air temperature better than the large wooden ones (SMHI types).

* Within the SMHI group the screen in bad condition performed worst, and the small screen was somewhat better than the large one in good condition.

* Within the group novel screens generally the Vaisala and Young agreed best with the reference.

The wind speed was very important. Above a wind speed of about 1 m/s (somewhat dependent upon the screen type and irradiation) the errors were close to 0. If it also was cloudy they were very close to 0.

With calm winds and clear weather without rapid and large air temperature changes the screen temperatures averaged about 0.5°C too high during day-time and about 0.5°C too low during the night.

Large absolute errors were most common about sunrise and sunset, coincident with considerable, rapid and 'regular' air temperature changes. With a clear sky and calm winds the errors became extreme (about +3°C and -2°C, somewhat better for the Vaisala screen).

Acknowledgements

Several employes of the Technical Division of SMHI have taken part in this project and made an excellent work. We have had valuable discussions with several persons from the Meteorological Division. We wish to express our deepest gratitude to all of them.

References

Fuchs, M. and C.B. Tanner: Radiation shields for air temperature measurements. J. Appl. Met., 4, 1965, 544-547.

Köppen, W.: Einheitliche Thermometeraufstillung für meteorologischen Stationen zur Bestimmung der Lufttemperatur und Luft-feuchtigkeit. Met. Zeitschr., 30, 1913, 474-488.

Middleton, W. E. K.: A History of the Thermometer and Its Use in Meteorology. The John Hopkins Press, Baltimore, Maryland, 1966, p 224 and 233.

Middleton, W. E. K. and A. F. Spilhaus: Meteorological Instruments. Third ed. Revised and reprinted 1960. Univ. Toronto Press, p 59.

Moden, H.: Beräkning av medeltemperaturen vid svenska stationer. Statens Meteorologisk-Hydrografiska Anstalt. Communications. Series of Papers, N:o 29, 1939. 12 p.

Sparks, W.,R.: The effect of thermometer screen design on the observed temperature. WMO - No.315, 1972. 106 p.

World Meteorological Organisation: Guide to meteorological instruments and methods of observation. Fifth edition. WMO - No.8, 1983, p 1.23, 4.3 .

World Meteorological Organization: Calculation of monthly and annual 30-year standard normals. Prepared by a meeting of experts, Washington, D.C., USA, March 1989. WCDP-No. 10, WMO-TD/No. 341.

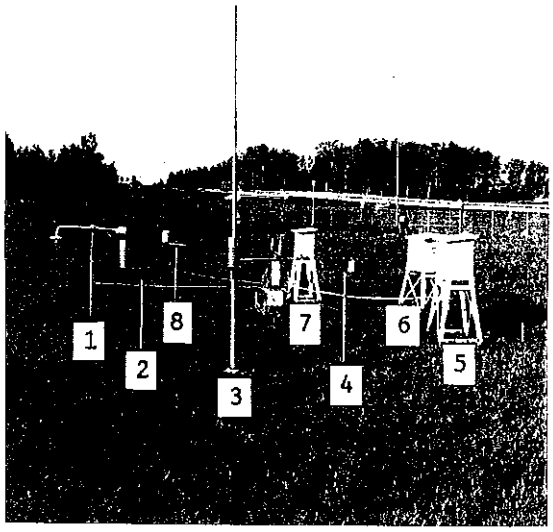

Fig 1. Photo of the test site. The numbers of the screens are shown. Oct 2, 1989, AM.

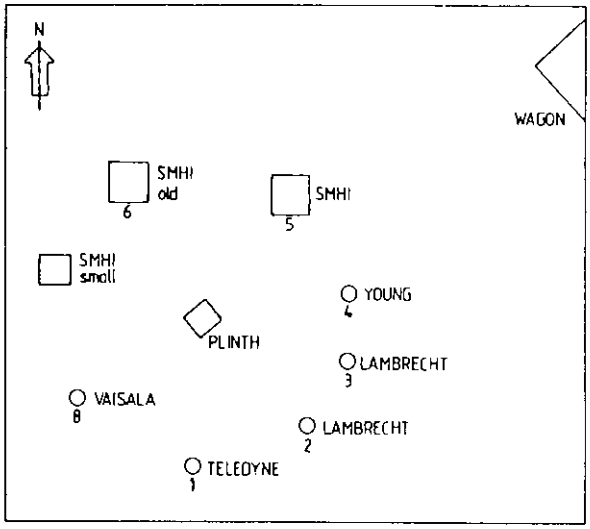

Fig 2. Map of the test site.

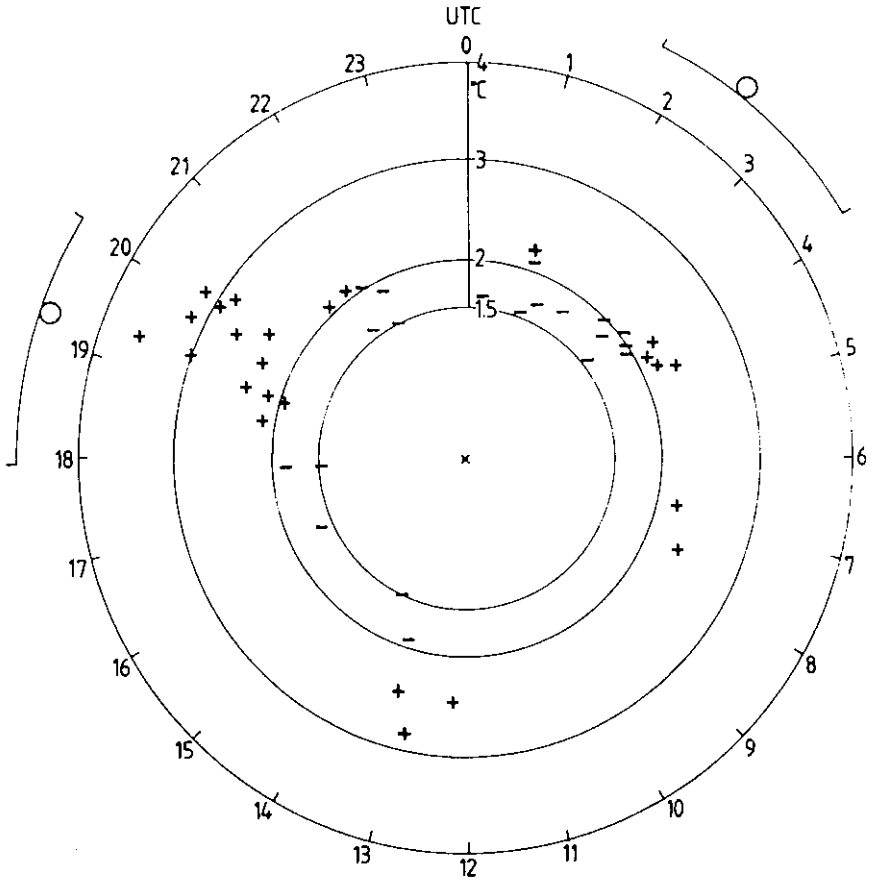

Fig 3. Polar diagram giving the time and magnitude of extreme DIFF. Mostly screen no 6 (SMHI screen in bad condition) is represented. Arcs outside the circles show the time of sunrise and sunset for April-August. Most extremes occur during summer and cluster about sunrise and sunset.
\+ DIFF >= 2.0°C
\- DIFF <= -1.5°C.

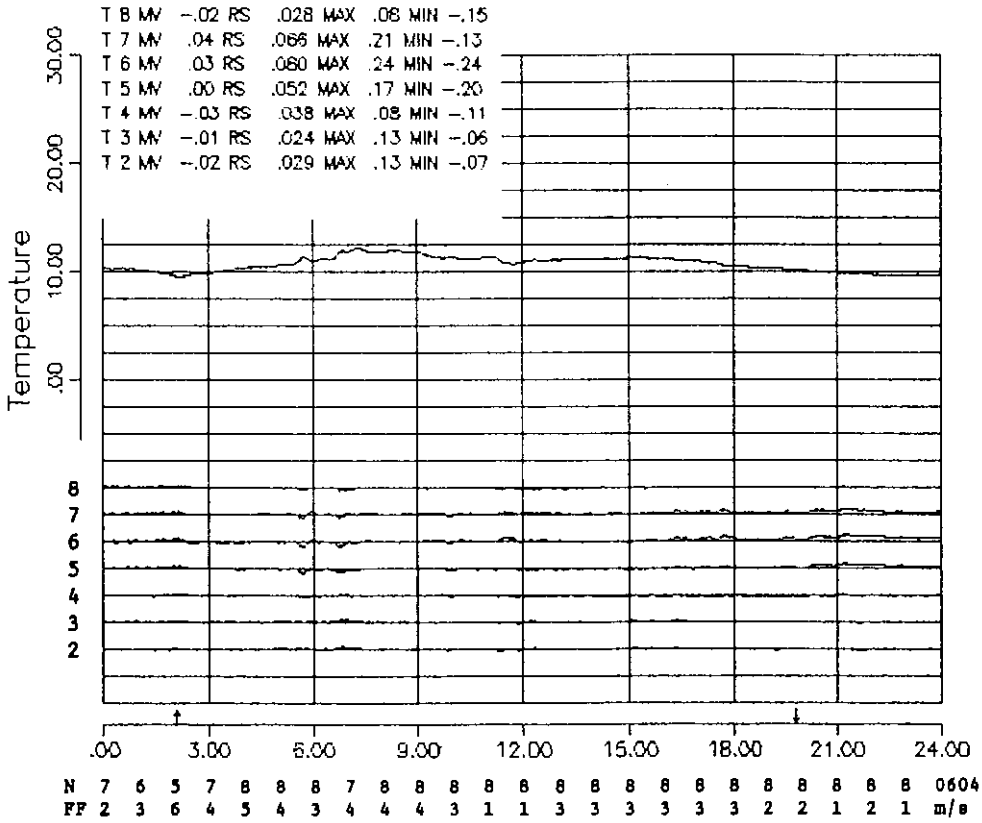

Fig 4a. Diurnal march of air temperature (according to the reference, screen no 1) and DIFF for a cloudy summer day with only slow air temperature changes, low-moderate wind and drizzle/light rain 11:10-13:15. The DIFFs are very close to zero and mostly lie on respectively axis. 890604.

Legend

The X axis gives time in UTC.
The Y axis gives air temperature and temperature differences, DIFF.

The upper curve gives air temperature according to the reference screen. The lower curves give DIFF. The Y scale there is 1°C. Each screen has its own zero line marked by its number. Counting downwards the screens are given in the order 8, 7, 6, 5, 4, 3 and 2, i e the same order as the statistics given in the upper left part of the Fig.

8 = VAISALA SCREEN
7 = small SMHI SCREEN
6 = ORDINARY SMHI SCREEN IN BAD CONDITION
5 = ORDINARY SMHI SCREEN IN GOOD CONDITION
4 = YOUNG SCREEN
3 = LAMBRECHT SCREEN, ON LONG POLE
2 = LAMBRECHT SCREEN, ON SHORT POLE

MV = arithmetic mean of the DIFF
RS = root mean square of the DIFF
MAX = maximum of the DIFF
MIN = minimum of the DIFF

N = total cloudiness in oktas from Bråvalla
FF = wind speed in m/s at anemometer level from Bråvalla

Times of sunrise and sunset are given by vertical arrows on the time scale.

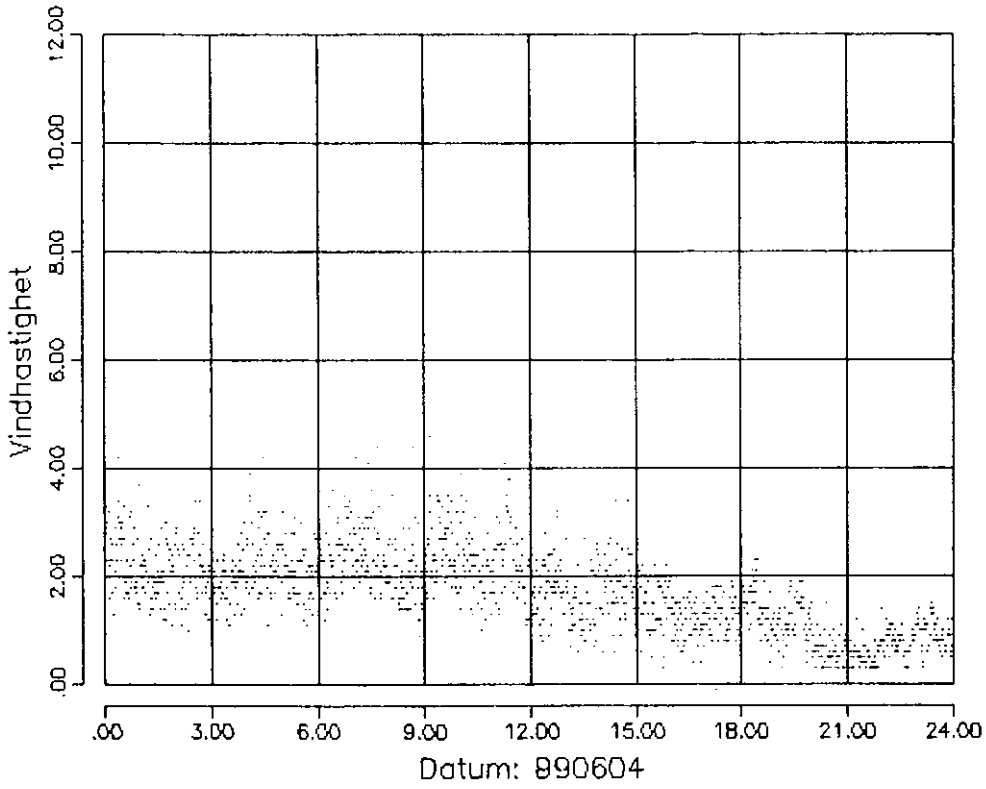

Fig 4b. Diurnal march of wind speed, m/s, at the level of the sensors, 890604.

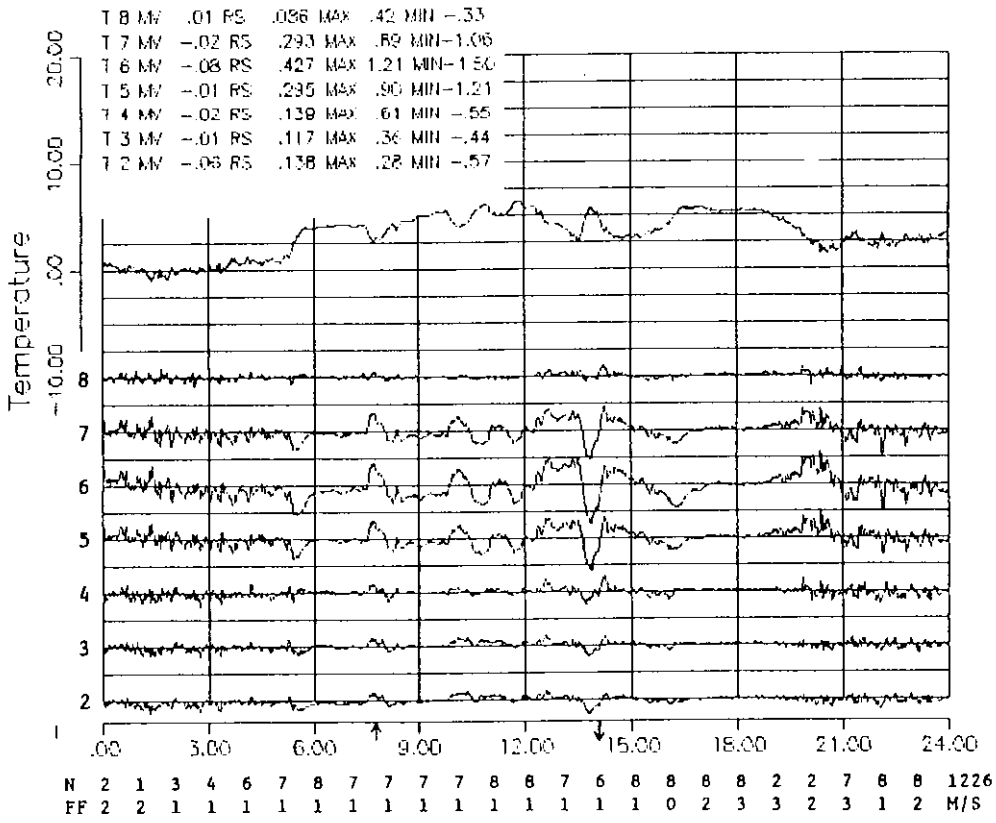

Fig 5a. Diurnal march of air temperature (reference) and DIFF for a cloudy winter day with rapid air temperature changes, bare ground and low winds. Note how slowly (expressed by large absolute DIFFs) the large screens (Nos 5-7) respond to rapid temperature changes. 891226. Legend, see Fig 4.

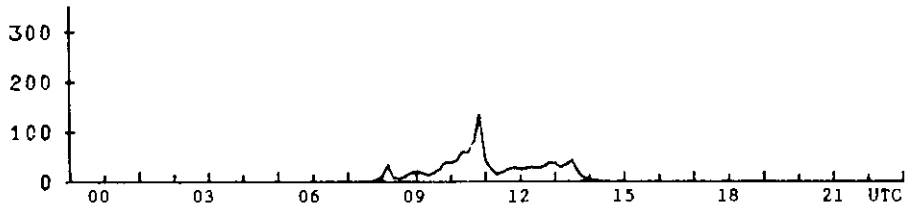

Fig 5b. Diurnal march of direct beam irradiance, W/m². 891226.

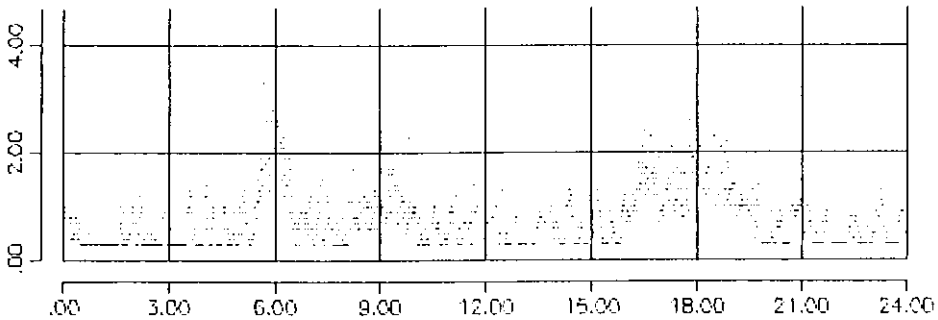

Fig 5c. Diurnal march of wind speed, m/s, at the level of the sensors. 891226.

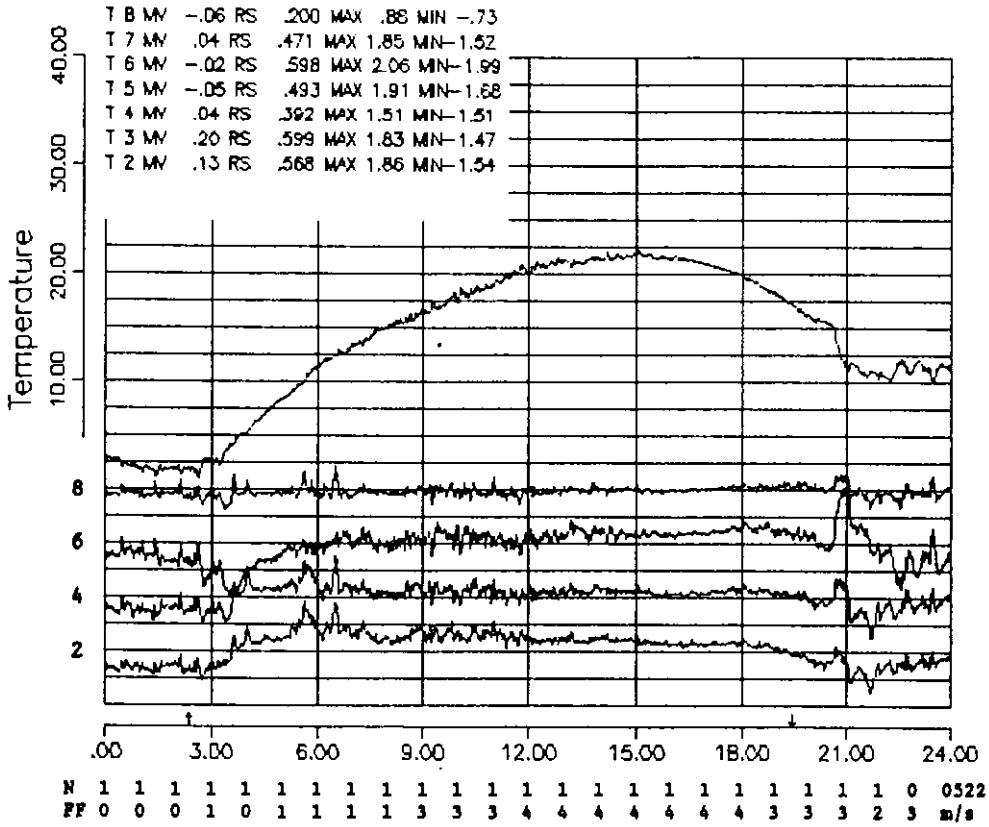

Fig 6a. Diurnal march of air temperature (reference) and DIFF for a clear spring day with calm and low winds. Wind speed (FF) in m/s at ordinary anemometer level. 890522. Legend, see Fig 4. For clarity only DIFF curves for (counting downwards) screens no 8, 6, 4 and 2 are drawn.

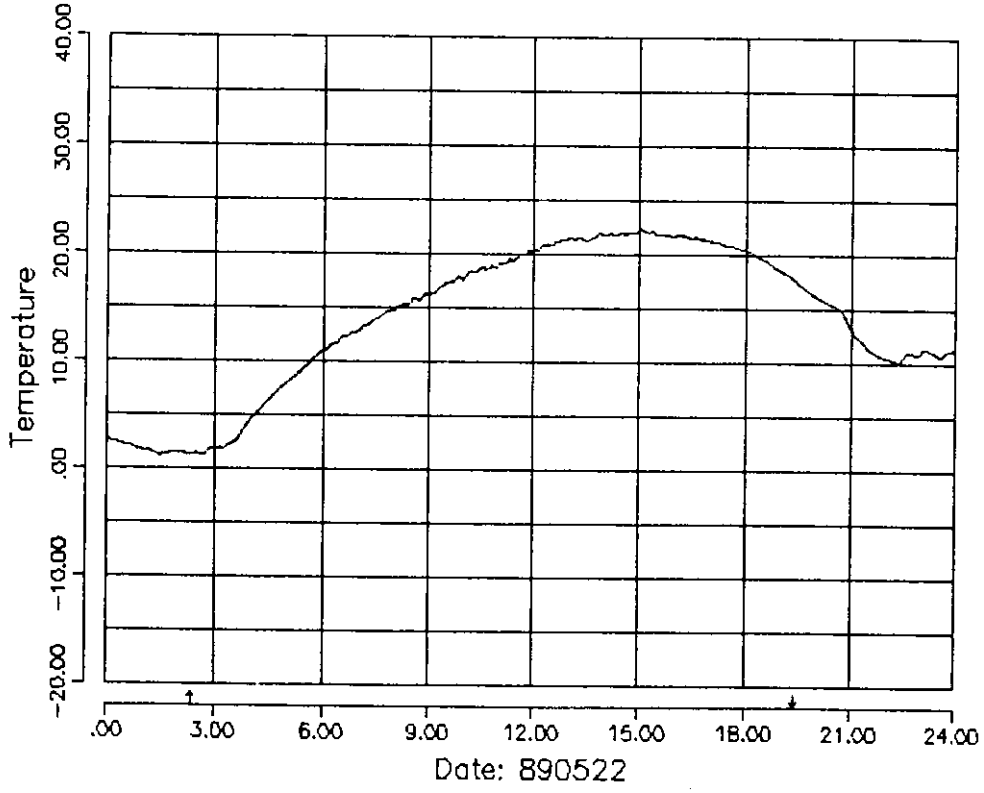

Fig 6b. Diurnal march of air temperature according to screen no 5 (SMHI, good condition). Note that the curve is much smoother than the corresponding one in Fig 5a. 890522.

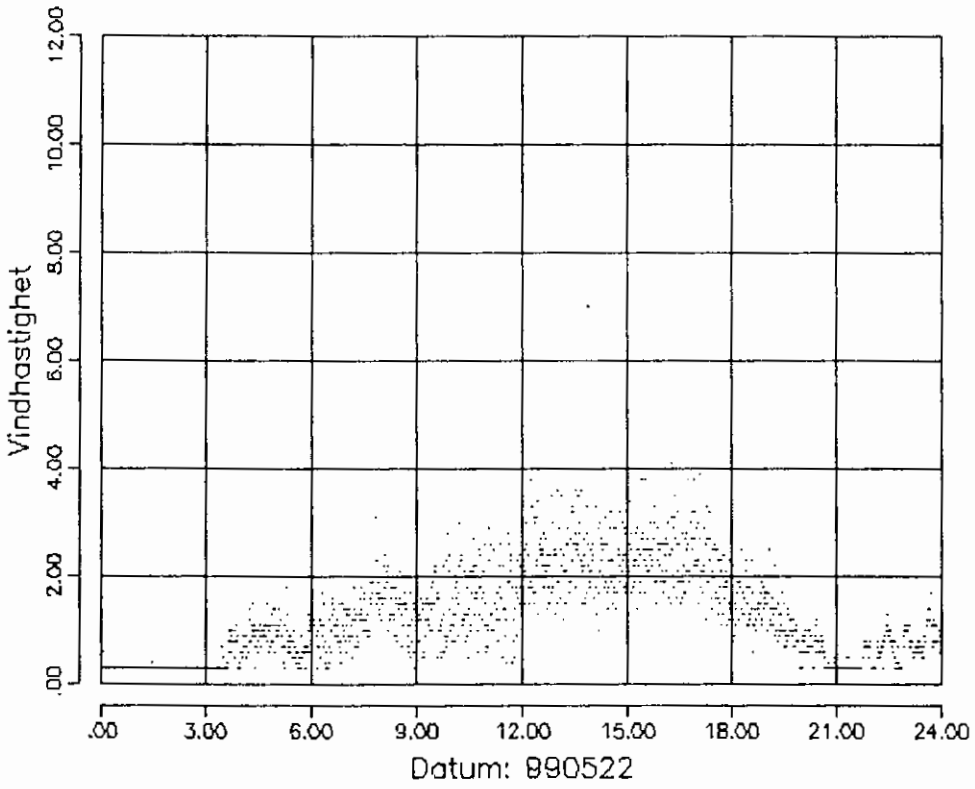

Fig 6c. Diurnal march of wind speed, m/s, at the level of the sensors. 890522.

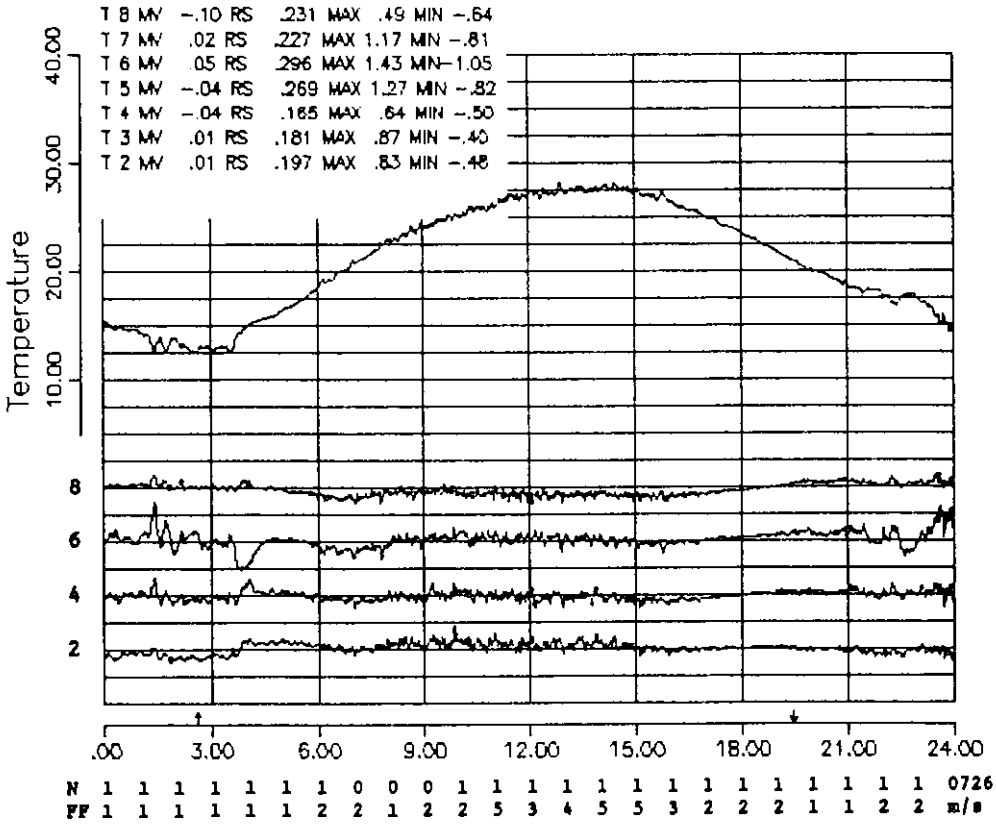

Fig 7a. Diurnal march of air temperature (reference) and DIFF for a clear summer day with moderate winds. 890726. Legend, see Fig 4. For clarity only DIFF curves for (counting downwards) screens no 8, 6, 4 and 2 are drawn.

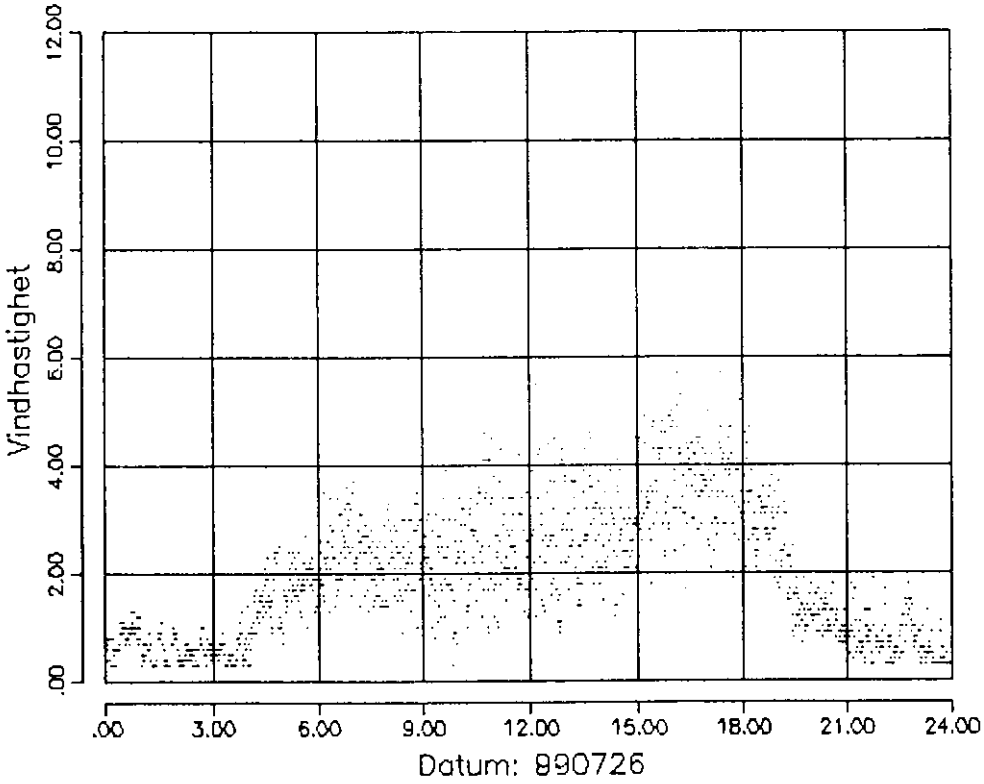

Fig 7b. Diurnal march of wind speed, m/s, at the level of the sensors. 890726.

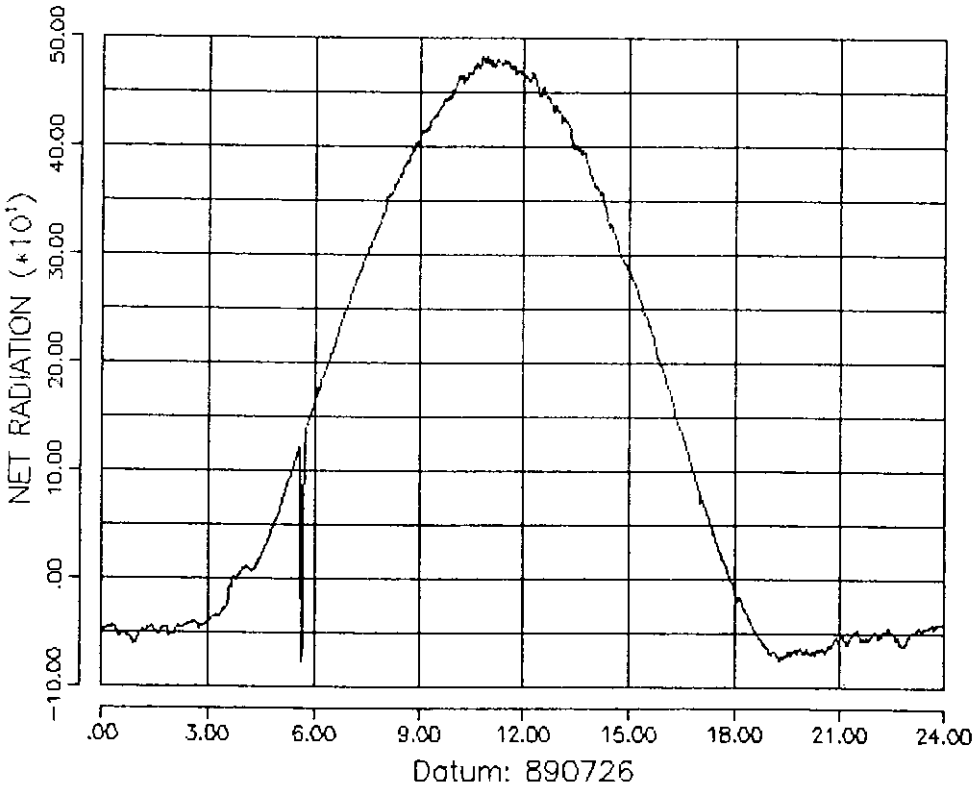

Fig 7c. Diurnal march of the net radiation, W/m², 890726. The 'spike' at about 05:30 is caused by the shadow from the pole of screen no 3.

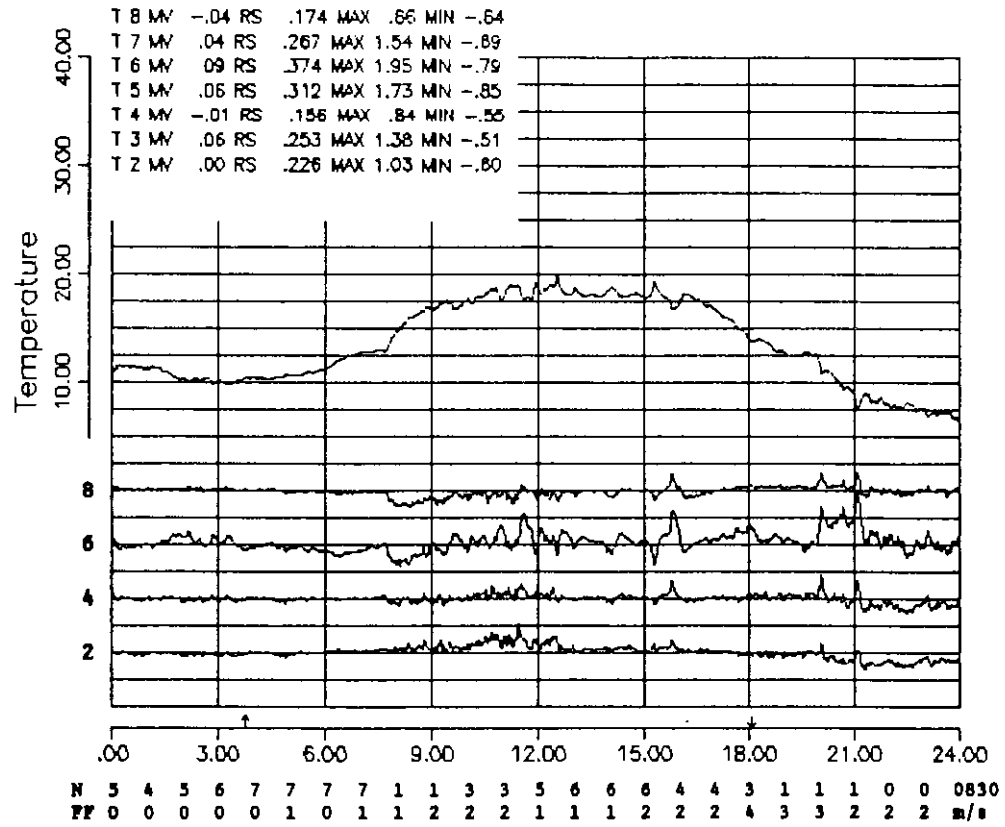

Fig 8a. Diurnal march of air temperature (reference) and DIFF for a summer day with varying cloudiness and low winds. 890830. Legend, see Fig 4. For clarity only DIFF curves for (counting downwards) screens no 8, 6, 4 and 2 are drawn.

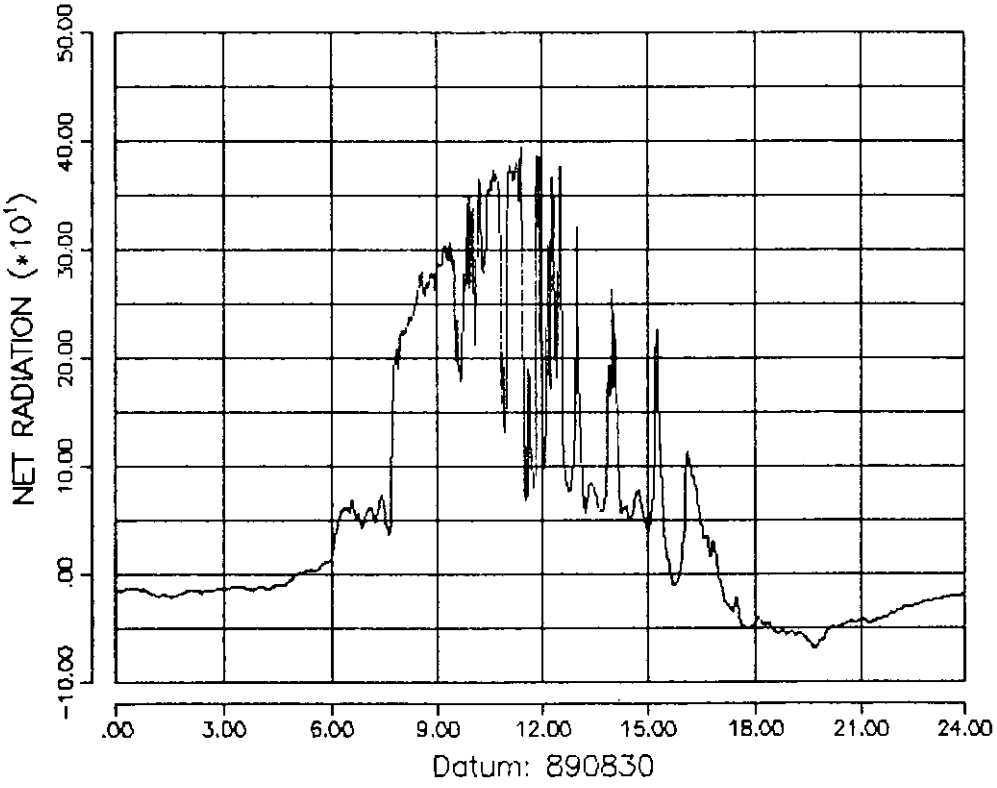

Fig 8b. Diurnal march of net radiation, W/m². 890830.

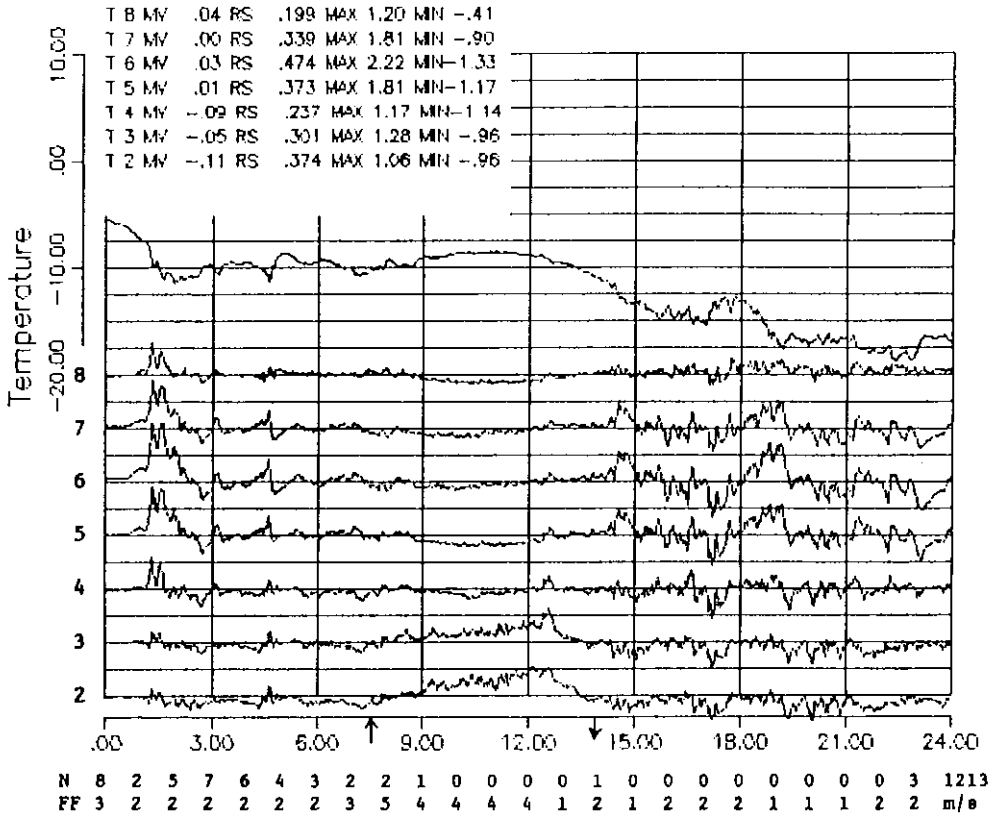

Fig 9a. Diurnal march of air temperature (reference) and DIFF for a clear winter day with snow cover and low winds. Note the long-lasting positive DIFFs for the Lambrechts (Nos 2 and 3) during day-time. 891213. Legend, see Fig 4.

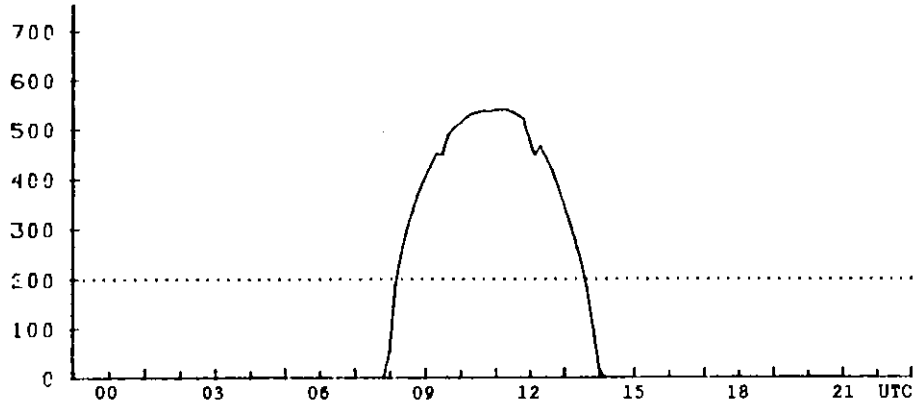

Fig 9b. Diurnal march of direct beam irradiance, W/m². 891213.

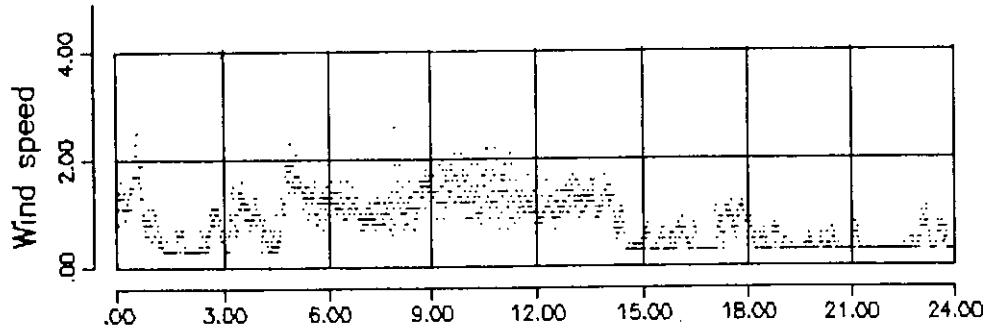

Fig 9c. Diurnal march of wind speed, m/s, at the level of the sensors. 891213.

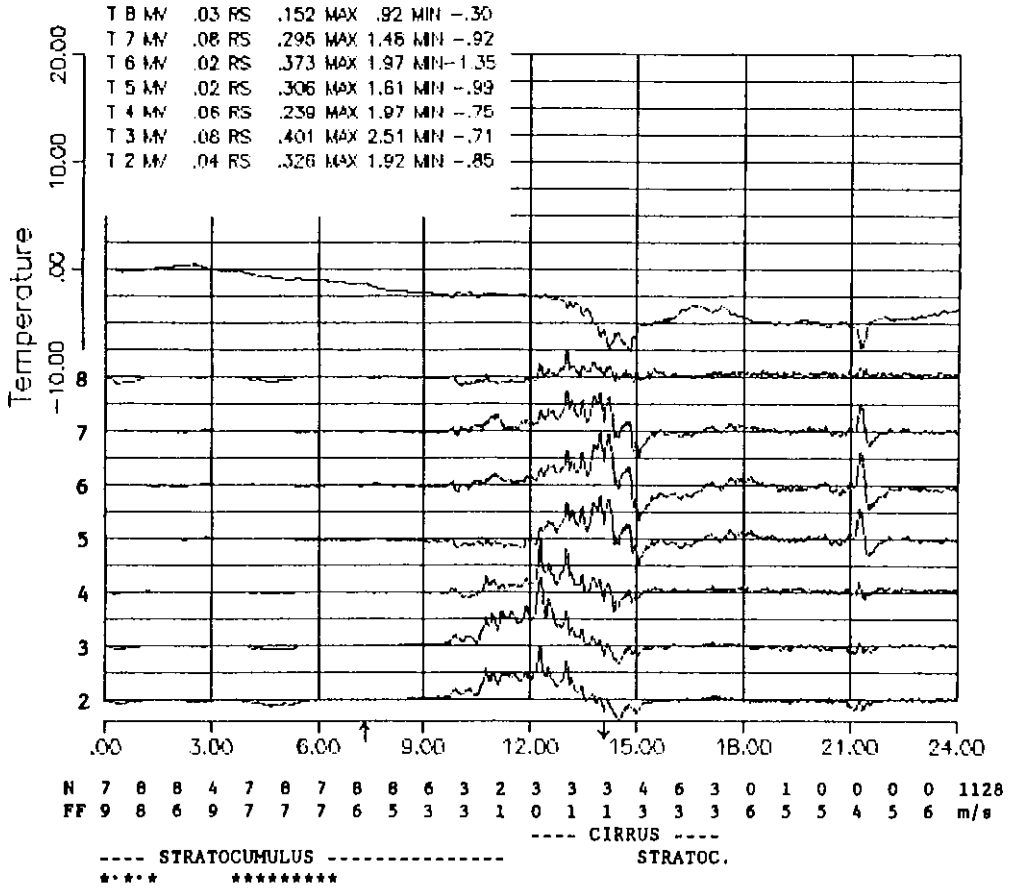

Fig 10a. Diurnal march of air temperature (reference) and DIFF for a clear winter day with fresh snow cover and low winds. Note the long-lasting positive DIFFs for the Lambrechts (Nos 2 and 3) during day-time. 891128. Legend, see Fig 4. * snow, *· snow and rain.

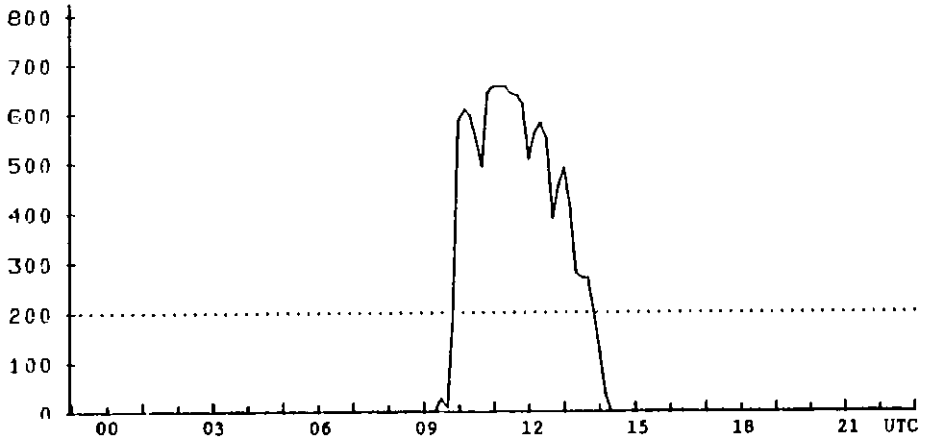

Fig 10b. Diurnal march of direct beam irradiance, W/m². 891128.

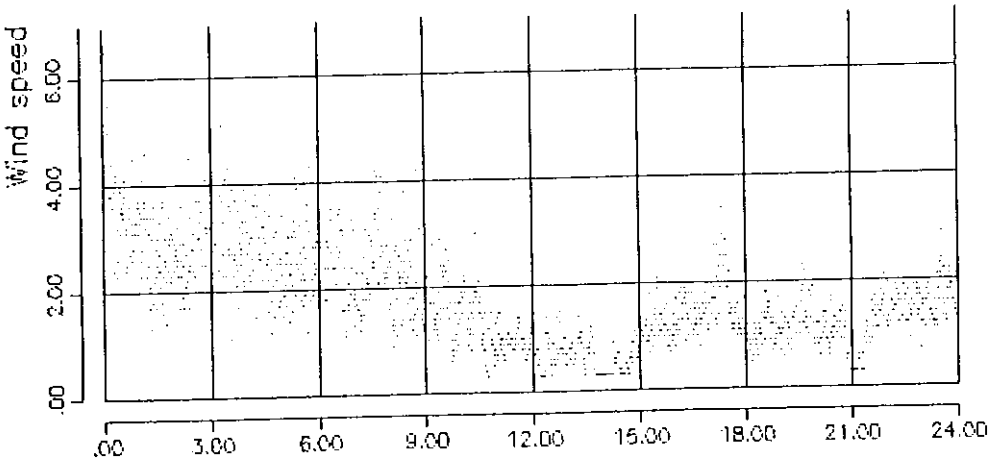

Fig 10c. Diurnal march of wind speed, m/s, at the level of the sensors. 891128.

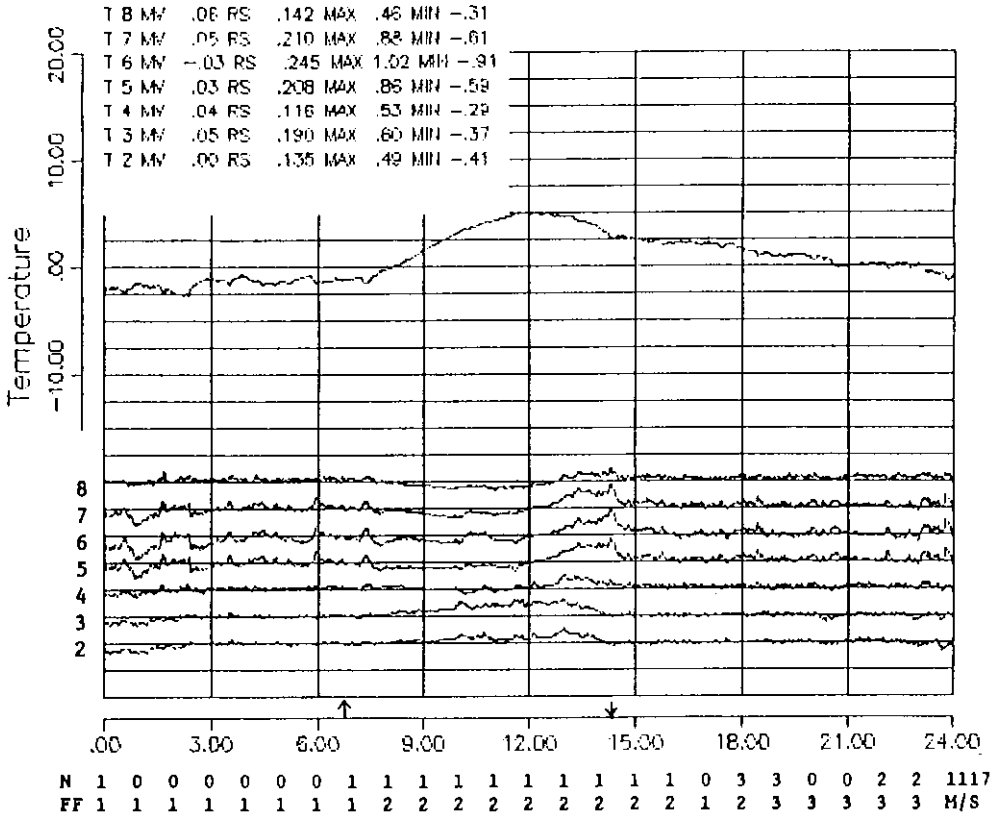

Fig 11a. Diurnal march of air temperature (reference) and DIFF for a clear autumn day with low winds and bare ground. 891117. Legend, see Fig 4.

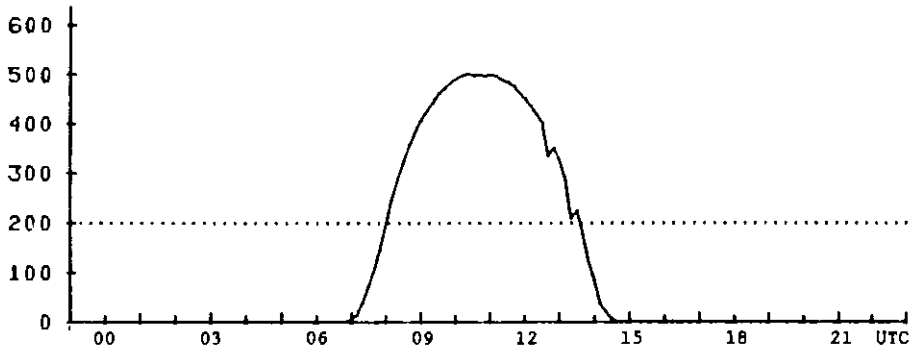

Fig 11b. Diurnal march of direct beam irradiance, W/m². 891117.

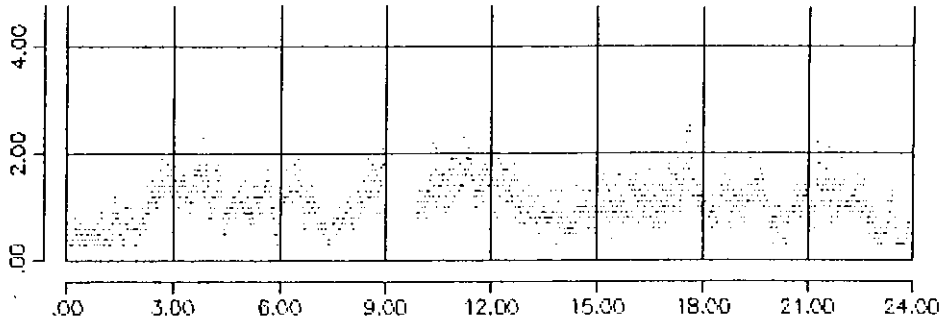

Fig 11c. Diurnal march of wind speed, m/s, at the level of the sensors. 891117.

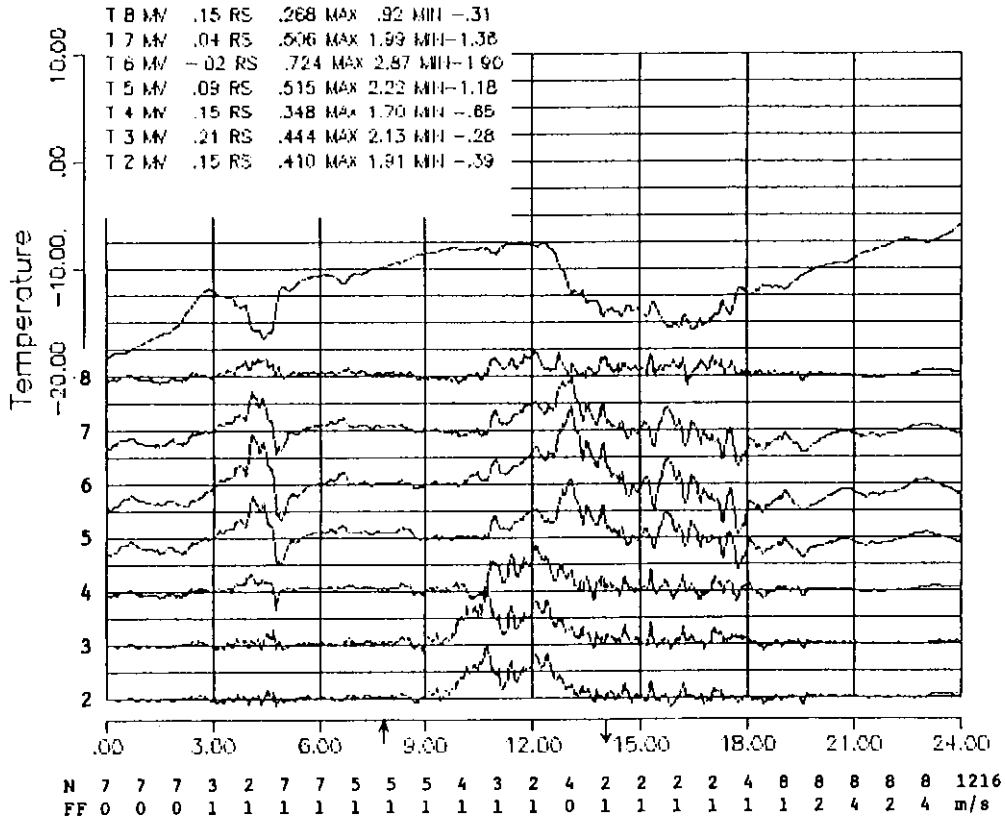

Fig 12a. Diurnal march of air temperature (reference) and DIFF for a clear winter day with low winds and snow cover. Note that though the Lambrechts (Nos 2 and 3) reacted to the irradiation earlier than the other screens, the latter also became overheated while the air temperature was nearly constant. The largest DIFFs for the SMHI screens (Nos 5-7) are caused by irradiation and a rapid air temperature drop. 891216. Legend, see Fig 4.

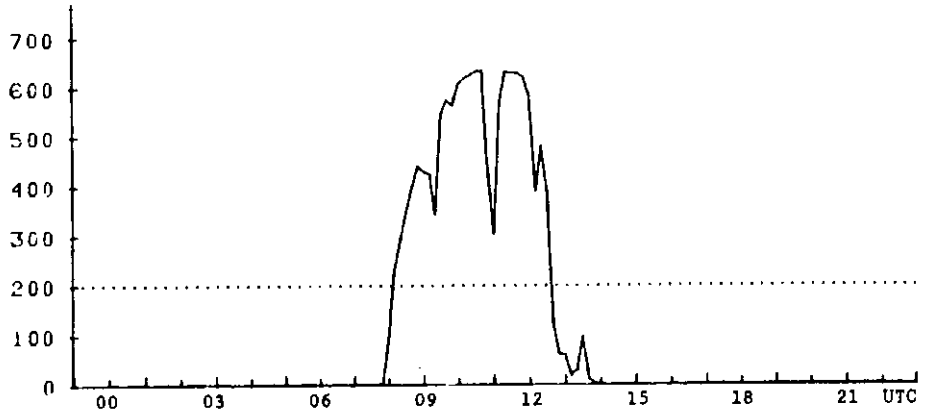

Fig 12b. Diurnal march of direct beam irradiance, W/m². 891216.

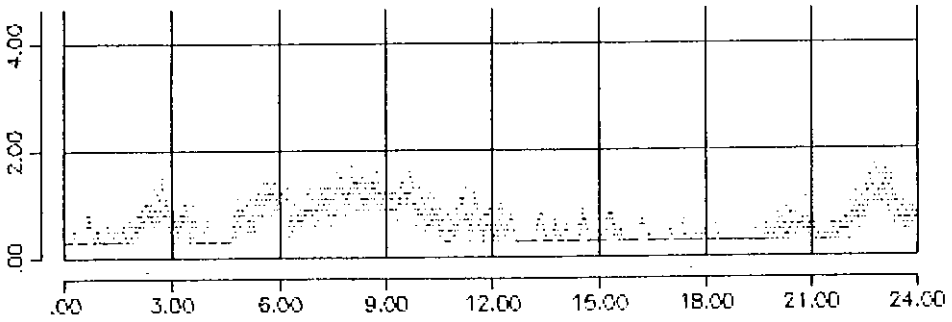

Fig 12c. Diurnal march of wind speed, m/s, at the level of the sensors. 891216.

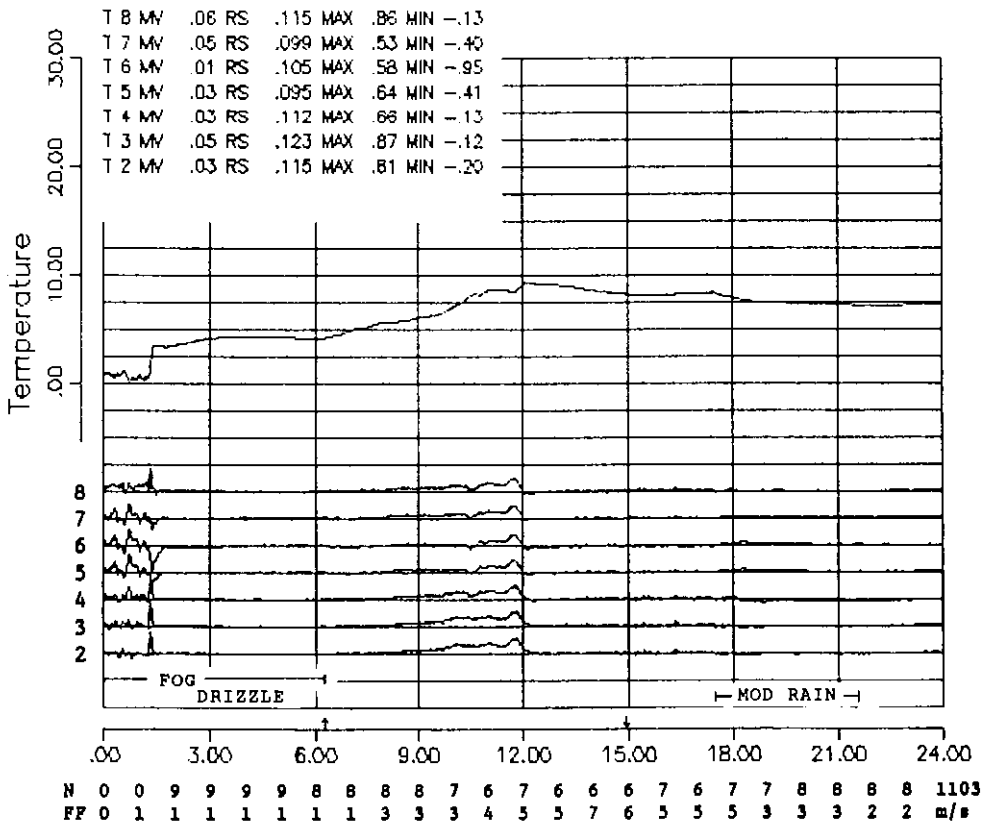

Fig 13a. Diurnal march of air temperature (reference) and DIFF for an autumn day with fog, drizzle and moderate rain. 891103. Legend, see Fig 4. Note the DIFFs during the rapid temperature rise and their character before and after it.

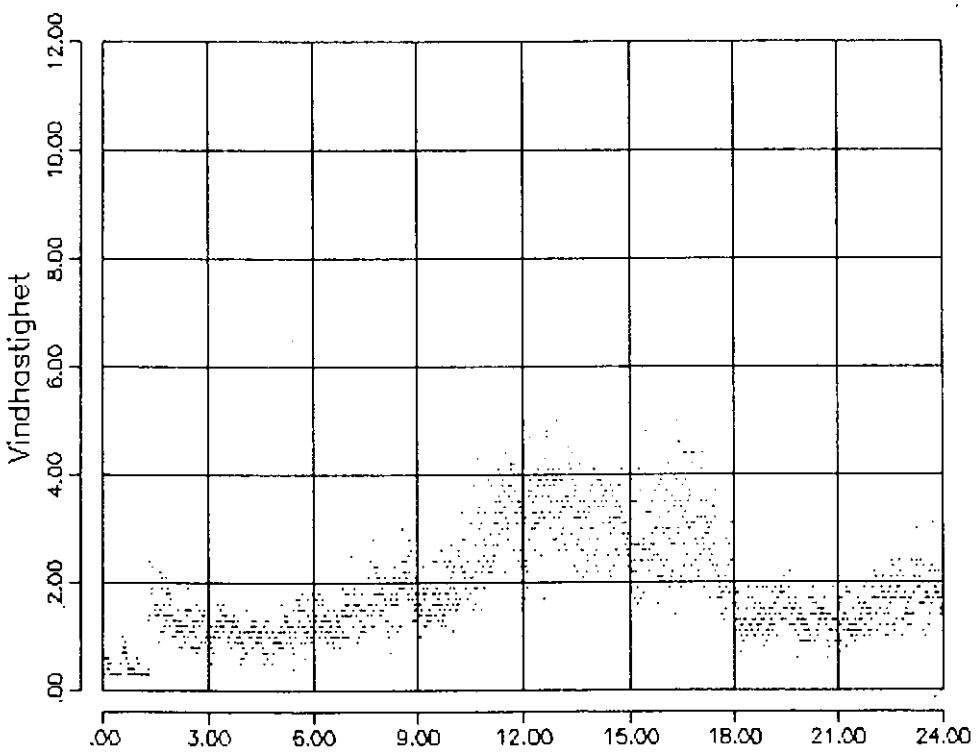

Fig 13b. Diurnal march of wind speed, m/s, at the level of the sensors. 891103.

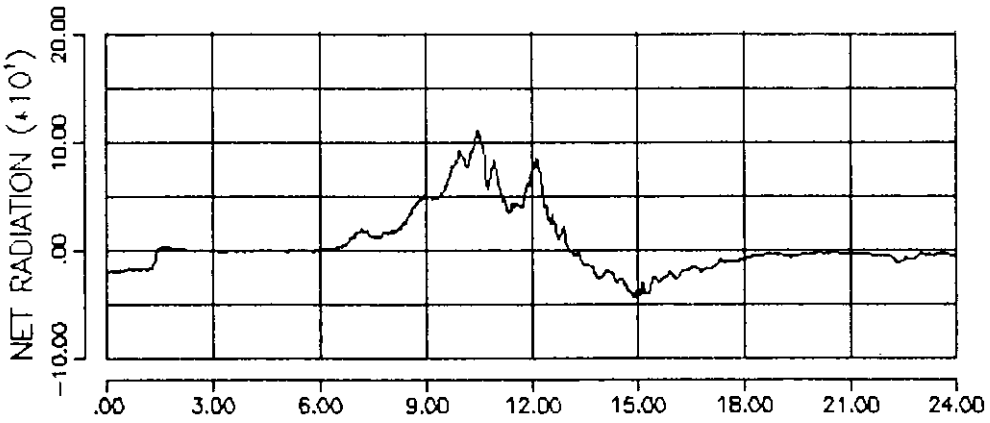

Fig 13c. Diurnal march of net radiation, W/m², 891103.

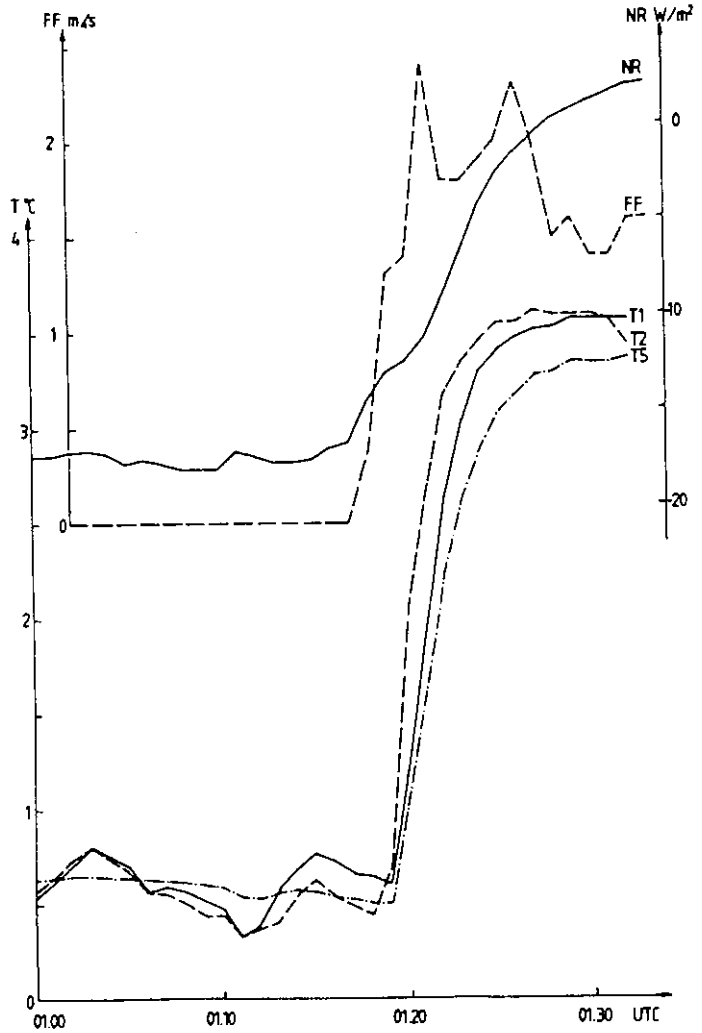

Fig 14. Some parameters during the rapid temperature rise 891103.
X coordinate is time in UTC.
T1 = air temperature according to the reference screen no 1
T2 = " " " " " Lambrecht " no 2
T5 = " " " " " SMHI " no 5
FF = wind speed at the level of the sensors
NR = net radiation.
Note that the Lambrecht screen (as well as the Young and Vaisala ones) responds faster to the temperature change than the reference.

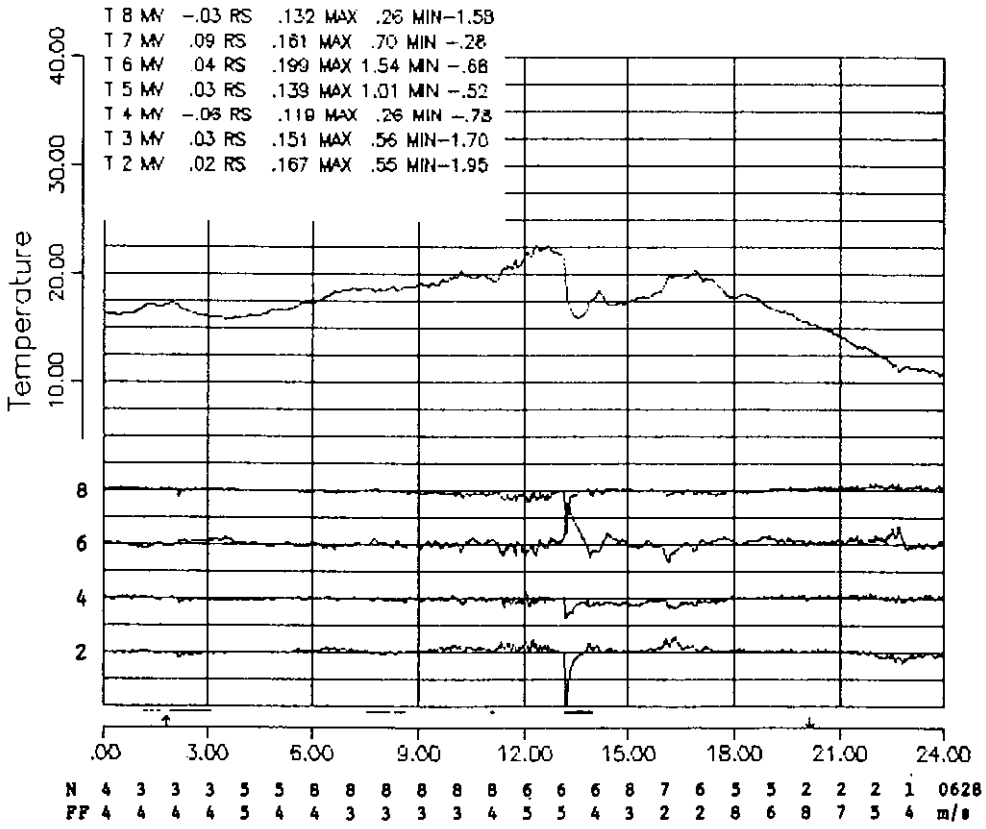

Fig 15a. Diurnal march of air temperature and DIFF for a summer day with showers. Solid horizontal line segments give time of precipitation. Only the shower just after 13:00 was heavy, with momentary rain rates about 1 mm/minute. Note the DIFF during that shower. For clarity only DIFF curves for (counting downwards) screens no 8, 6, 4 and 2 are drawn. 890628. Legend, see Fig 4.

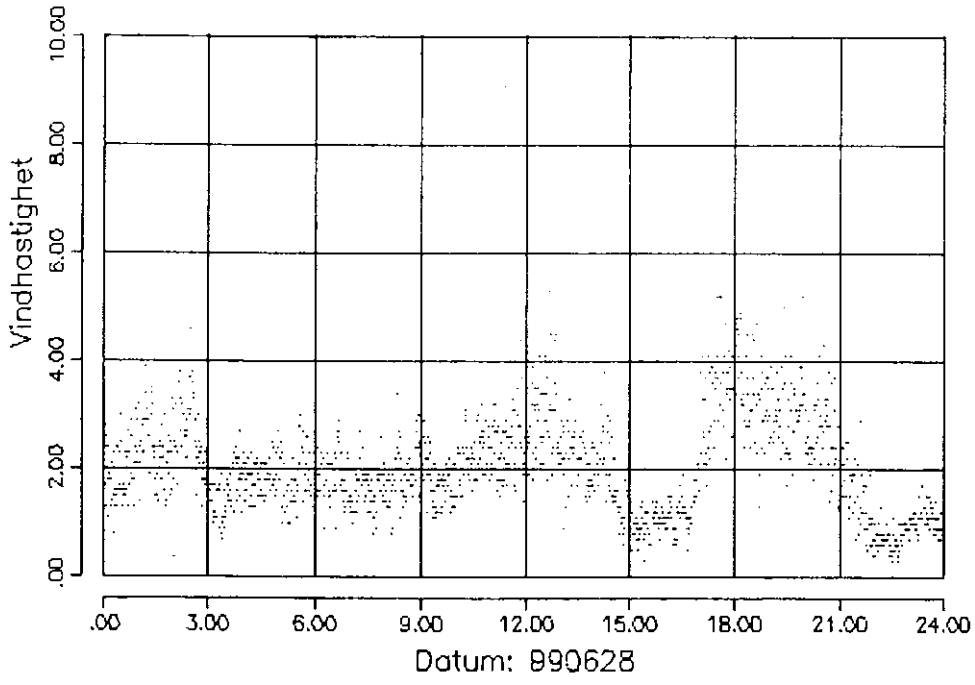

Fig 15b. Diurnal march of wind speed at the level of the sensors. 890628.

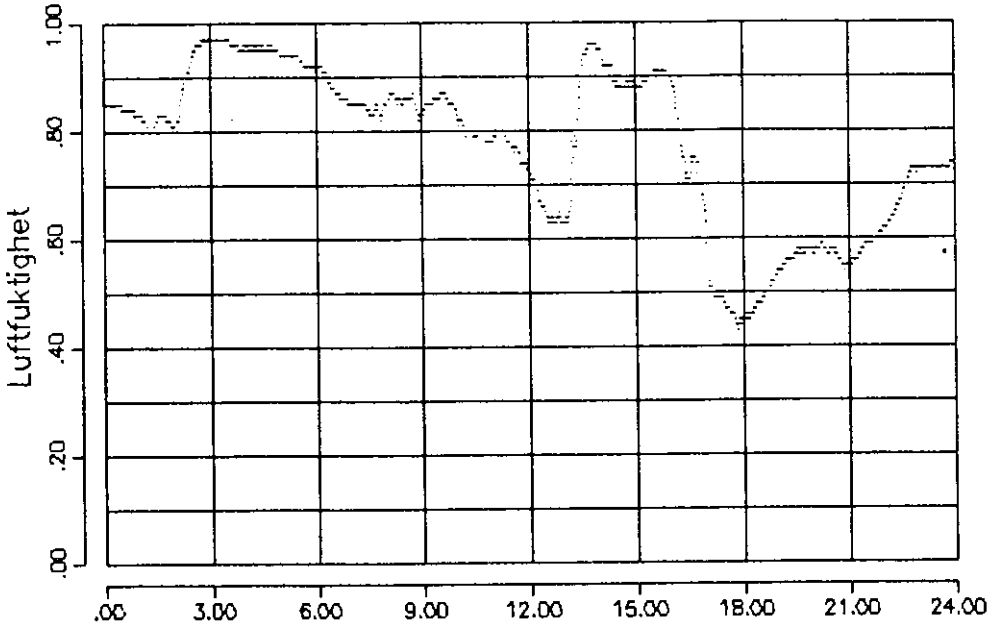

Fig 15c. Diurnal march of the relative humidity. 890628.

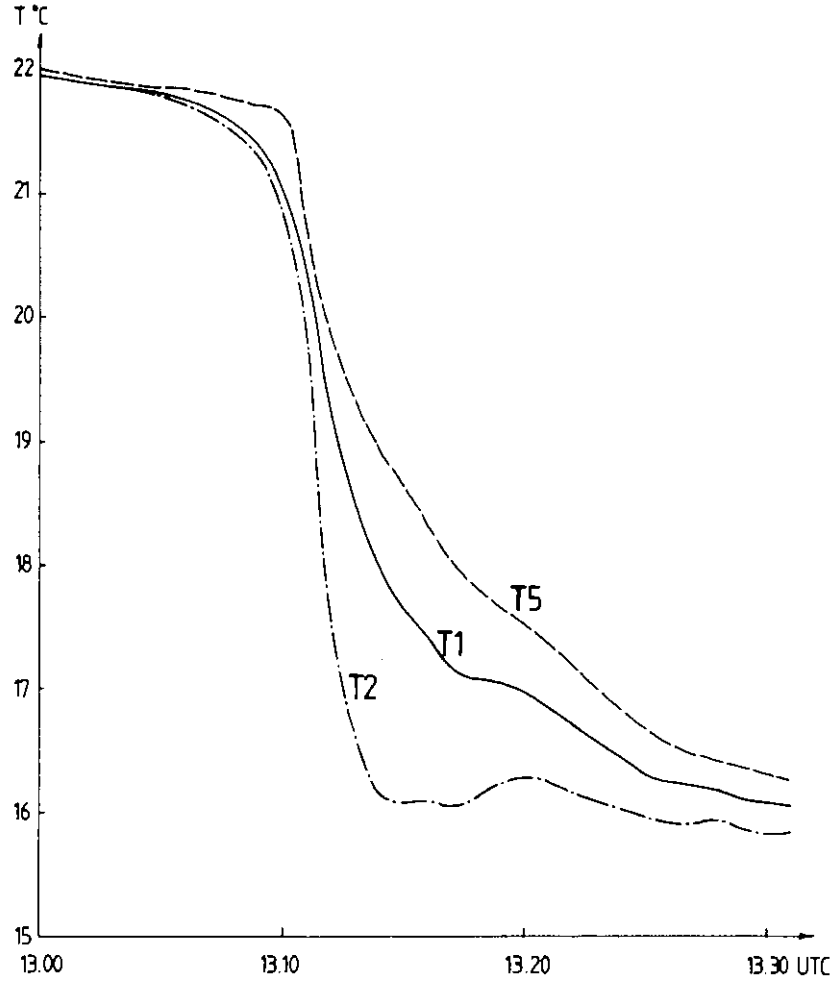

Fig 16. Air temperature according to the reference screen (T1), the Lambrecht screen no 2 (T2) and the SMHI screen no 5 (T5) during the heavy shower 890628.

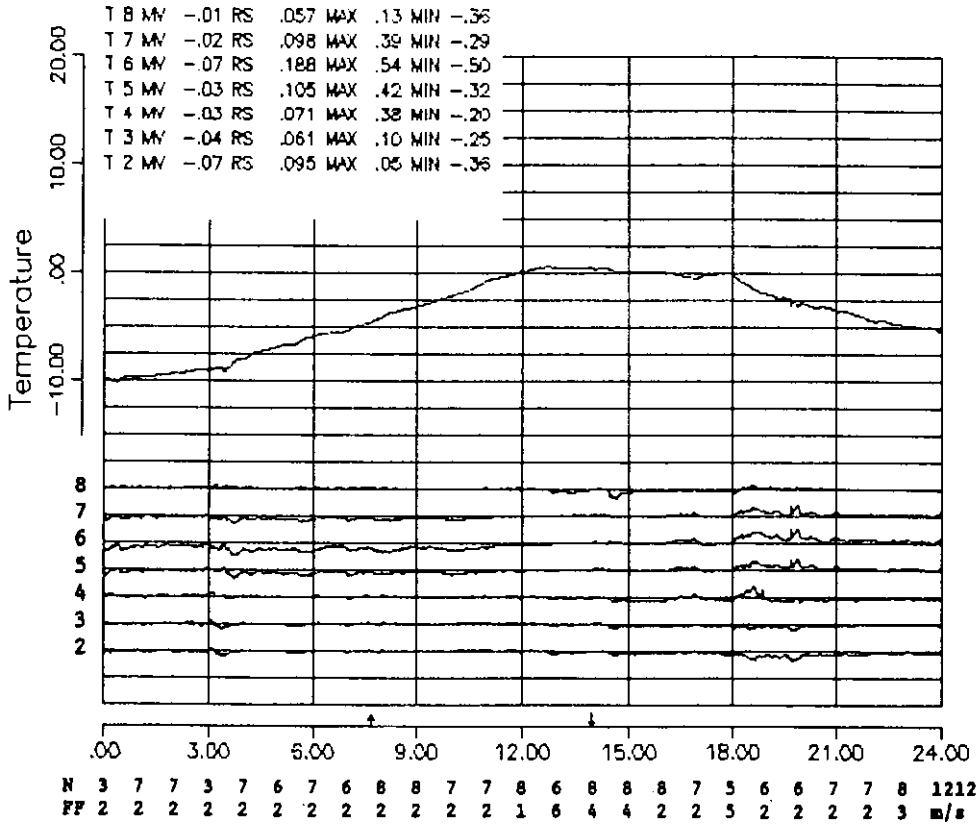

Fig 17. Diurnal march of air temperature (reference) and DIFF for a cloudy winter day with snowfall. 891212. Legend, see Fig 4.

- Motor aspirated
- Triple-shielded enclosure
- Accepts a wide selection of sensing elements
- Built-in access to temperature probe
- Accessory dew point and relative humidity sensor adapter

motor-aspirated thermal radiation shield

For critical measurements of atmospheric temperature and temperature gradients, Geotech offers the Motor-Aspirated Thermal Radiation Shield, Model 327C. This patented device shields temperature sensors against the effects of solar and terrestrial radiation so effectively that sensor error does not exceed 0.05°C in any temperature range or at any radiation angle under radiation intensities encountered anywhere on earth.

To achieve this level of radiation immunity, the Model 327C uses a unique combination of baffles and shields to protect the sensor cavity. The cavity is first surrounded by a thin cylindrical shield of stainless steel, with a high surface-to-mass ratio. Surrounding the inner shield is a second cylindrical shield manufactured of heavy-gauge aluminum. This shield serves to protect the inner shield and is of a different material to reduce the effects of secondary emissions. Removal of the last perceptible direct radiation error is accomplished by the addition of an umbrella shield that protects the cylindrical shields during periods of maximum solar radiation intensity.

The sensor cavity is continuously aspirated by means of a forced-air blower mounted at the opposite end of the support arm. This artificial aspiration ensures that fresh air samples, whose temperature is that of the surrounding atmosphere, are brought into the cavity independently of prevailing wind conditions.

The air intake is carefully baffled to eliminate errors caused by reflected or terrestrial radiation and to ensure that air samples are drawn from the elevation of the intake with minimum vertical disturbance.

Since continuous aspiration is required for proper measurement, a failure warning detector is provided. This device consists of an air-flow actuated vane with a SPDT reed switch whose contacts close whenever air flow ceases.

MODEL 327C

The Teledyne ventilated screen.

SPECIFICATIONS - 327C

OPERATING CHARACTERISTICS

Shielding	Under test radiation flux density of 1100 W/m² (1.6 cal/cm² min) errors caused by radiation are less than 0.1°C (0.05°F)
Aspiration Rate	3 m/sec (10 ft/sec) at sensor location
Power	Aspirator motor requires 0.65A at 115 V, 60 Hz (220 V, 50 Hz or 12 Vdc on special order)

ENVIRONMENTAL CHARACTERISTICS

Operating temperature	–40°C to +65°C (–40°F to +150°F)
Finish	Reflective white enamel
Air Flow Detector	Factory-installed device for detection of aspirator air flow failure

OPTIONS

Dew Point/ Relative Humidity	Adapters for lithium-chloride and cooled-mirror sensors

PHYSICAL CHARACTERISTICS

Weight	6.8 kg (15 lb)
Shipping Data	
Weight	11.8 kg (26 lb)
Volume	0.5 m³ (18 ft³)

TELEDYNE GEOTECH
P.O. BOX 469007/GARLAND, TEXAS 75046-9007
3401 SHILOH RD./(214) 271-2561/TELEX 732394

JANUARY 1984/M 112

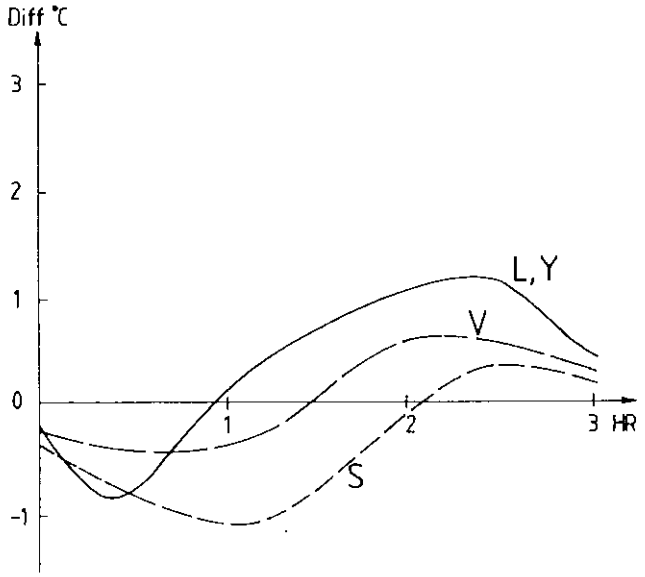

Fig 18. The sunrise effect on screen temperature.
Zero on the time scale is time of sun-rise.
S = SMHI type
L = Lambrecht type
Y = Young type
V = Vaisala type.

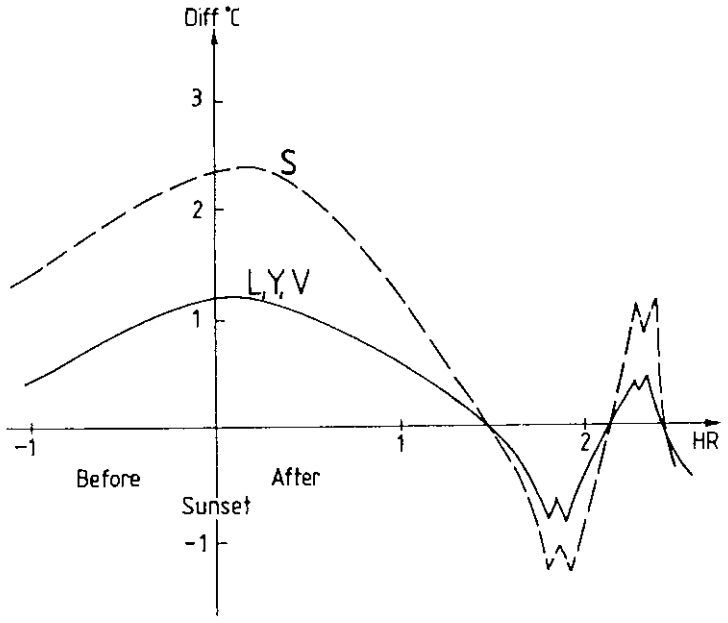

Fig 19. The sunset effect on screen temperature.
Zero on the time scale is time of sun-set.
S = SMHI type
L = Lambrecht type
Y = Young type
V = Vaisala type.

GILL MULTI-PLATE RADIATION SHIELD

The Gill Multi-Plate Radiation Shield is a naturally ventilated shield designed for ambient temperature, dew point temperature, and relative humidity sensors. The convenient size and light weight of this shield make it useful for a wide range of applications. It is especially well suited for field studies where power is limited.

Different sensor mounting configurations allow the shield to accommodate most commercially available temperature sensors. Several commonly used dew point and relative humidity sensors can also be easily mounted in this shield. Sensors are mounted vertically within the shield.

Model 41002 has a 1 inch standard tapered pipe thread for sensor mounting. A matching threaded hex plug is used to hold the sensor. When specified with the order, this fitting is predrilled to accommodate the desired sensor. If the sensor is not specified, an undrilled fitting is provided. Model 41004 has a 33 mm (1.30 in) I.D. cavity which accepts several types of sensor mounting adapters. A Universal Sensor Adapter is normally supplied for mounting sensors up to 10 mm (0.39 in) diameter. For larger diameters up to 26 mm (1.02 in) a Probe Adapter Ring is substituted. Two small screw clamps are used to hold the sensor adapter in position. Both radiation shield models have an offset type mounting bracket with a V-block and U-bolt which allows the shield assembly to be easily attached to a vertical pipe of any diameter between 25-50 mm (1-2 in). This mounting configuration permits easy access for sensor installation and servicing.

Twelve white opaque molded plastic discs permit easy air passage through the shield but the unique disc profile provides positive blockage of direct and reflected solar radiation. The thermoplastic disc material is a special formulation for maximum weatherability. This material provides high reflectivity, low thermal conductivity, and low heat retention.

The shield assembly is 12 cm diameter by 27 cm overall height. The twelve shield discs are mounted on three support studs with 11 mm separation between plates.

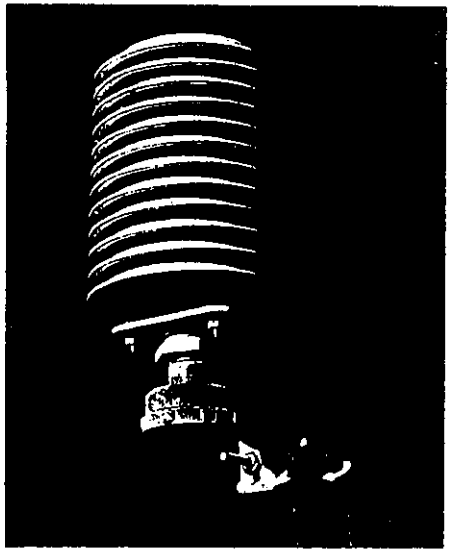

Wind tunnel tests with artificial radiation indicate that under conditions of low air movement (1 m/s) and maximum solar radiation, the temperature sensor is maintained within 1.5C° of ambient. With winds at 2 m/s the error is reduced to less than 0.7C° and with winds of 3 m/s the error is 0.4C° or less. These results have been independently verified in field tests.

SPECIFICATIONS: MODEL 41002/41004 MULTI-PLATE RADIATION SHIELD

SENSOR CLEARANCE:
- Model 41002 – 29 mm (1.14 in) diameter x 12 cm (4.7 in) length
- Model 41004 – 32 mm (1.26 in) diameter x 12 cm (4.7 in) length

RADIATION ERROR:
- Under radiation intensity of 1080 W/m²
- Dependent upon wind speed (ventilation rate) –
  - 0.4C° (0.7F°) RMS @ 3 m/s (6.7 mph)
  - 0.7C° (1.3F°) RMS @ 2 m/s (4.5 mph)
  - 1.5C° (2.7F°) RMS @ 1 m/s (2.2 mph)

MATERIAL:
- White thermoplastic UV stabilized for long term weatherability
- Gloss white painted aluminum mounting bracket (with molded plastic V-block and stainless steel U-bolt)

DIMENSIONS:
- Overall – 12 cm (4.7 in) diameter x 27 cm (10.6 in) height
- Plates – 2 mm (0.08 in) thick x 11 mm (0.44 in) spacing

MOUNTING:
- V-block and U-bolt fit vertical pipe 25-50 mm (1-2 in) diameter

WEIGHT:
- Net Weight – 0.7 kg (1.4 lbs)
- Shipping Weight – 1.4 kg (3 lbs) approx.

The Young screen.

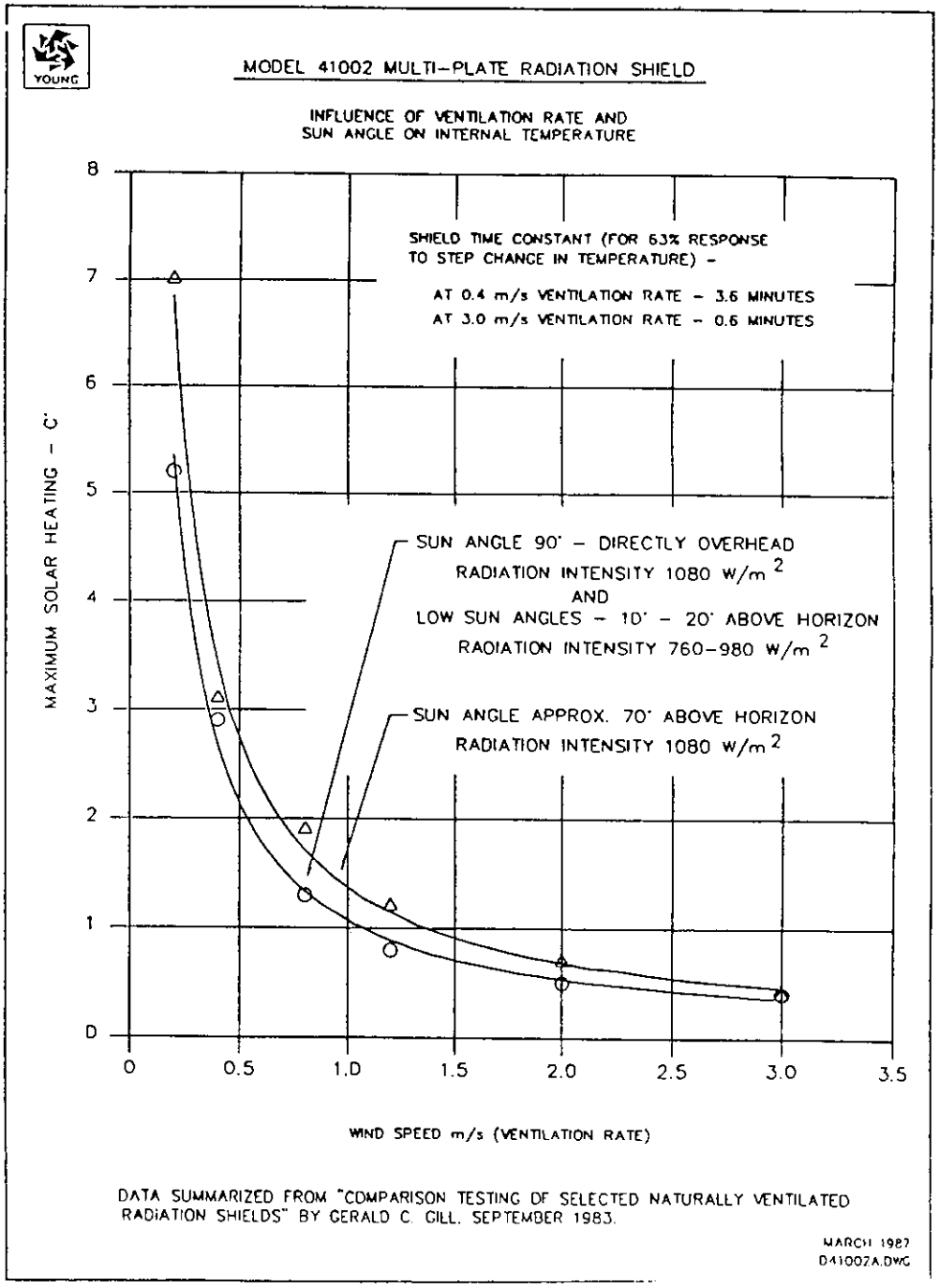

814
Schutzhütte, Niederschlags- und Strahlungshütte für die Geräte 800 . . . und 809 . . .; aus wetterfestem Aluminium, eloxiert.

Abmessungen: Höhe 440 mm, Durchmesser 170 mm, Durchmesser des Montagezapfens 22 mm
Gewicht: ca. 1,7 kg

The Lambrecht screen.

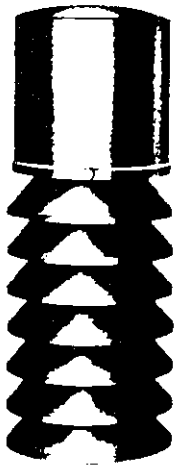

814

RADIATION SHIELD DTR 11

This radiation shield protects environmental sensors against direct solar radiation and precipitation.

It can house almost any type of temperature and humidity transducers thanks to its flexible fastening construction.

The shield is made of fiber glass reinforced polyester. The surface is UV-stabilized to withstand solar exposure. The surfaces receiving direct radiation are white to reflect the energy, while inside surfaces are black in order to absorb accumulated heat. The shield is maintenance-free.

TECHNICAL DATA
Outside dimensions
– **diameter** 220 mm
– **height** 292 mm
Inside dimensions
– **diameter** 110 mm
– **height** 223.5 mm
Weight 1.9 kg
Installation
– **max. clamping diameter** 70 mm
– **min. clamping diameter** 35 mm

The Vaisala screen.

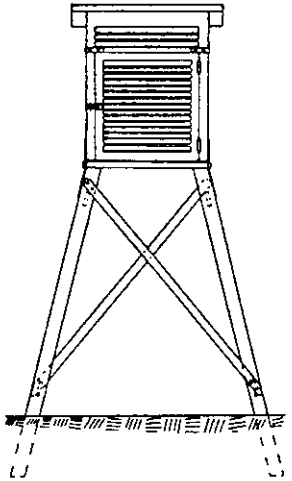

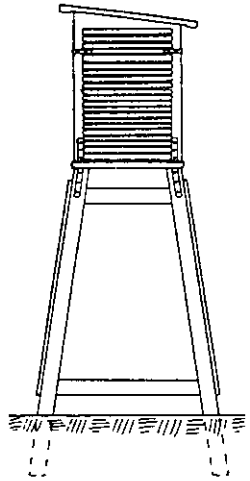

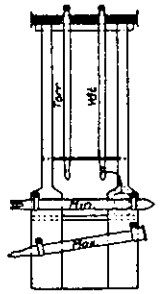

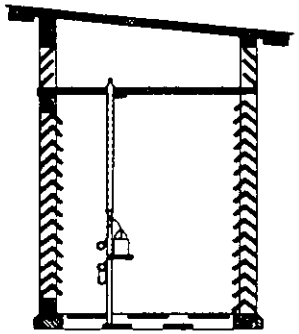

The SMHI screen. The screens have a double roof.

The large screen has width=70 cm, depth=40 cm and height=81 cm.

The corresponding figures for the small one are 40, 40 and 68 cm.

SMHI
HO
kuy/L/SCR

SMHI Rapporter, METEOROLOGI OCH KLIMATOLOGI (RMK)

Nr 1 Thompson, T, Udin, I, and Omstedt, A
Sea surface temperatures in waters surrounding Sweden.
Stockholm 1974

Nr 2 Bodin, S
Development on an unsteady atmospheric boundary layer model.
Stockholm 1974

Nr 3 Moen, L
A multi-level quasi-geostrophic model for short range weather predictions.
Norrköping 1975

Nr 4 Holmström, I
Optimization of atmospheric models.
Norrköping 1976

Nr 5 Collins, W G
A parameterization model for calculation of vertical fluxes of momentum due to terrain induced gravity waves.
Norrköping 1976

Nr 6 Nyberg, A
On transport of sulphur over the North Atlantic.
Norrköping 1976

Nr 7 Lundqvist, J-E, and Udin, I
Ice accretion on ships with special emphasis on Baltic. conditions
Norrköping 1977

Nr 8 Eriksson, B
Den dagliga och årliga variationen av temperatur, fuktighet och vindhastighet vid några orter i Sverige.
Norrköping 1977

Nr 9 Holmström, I, and Stokes, J
Statistical forecasting of sea level changes in the Baltic.
Norrköping 1978

Nr 10 Omstedt, A, and Sahlberg, J
Some results from a joint Swedish-Finnish sea ice experiment, March, 1977.
Norrköping 1978

Nr 11 Haag, T
Byggnadsindustrins väderberoende, seminarieuppsats i företagsekonomi, B-nivå.
Norrköping 1978

Nr 12 Eriksson, B
Vegetationsperioden i Sverige beräknad från temperaturobservationer.
Norrköping 1978

Nr 13 Bodin, S
En numerisk prognosmodell för det atmosfäriska gränsskiktet grundad på den turbulenta energiekvationen.
Norrköping 1979

Nr 14 Eriksson, B
Temperaturfluktuationer under senaste 100 åren.
Norrköping 1979

Nr 15 Udin, I, och Mattisson, I
Havsis- och snöinformation ur datorbearbetade satellitdata - en modellstudie.
Norrköping 1979

Nr 16 Eriksson, B
Statistisk analys av nederbördsdata. Del I. Arealnederbörd
Norrköping 1979.

Nr 17 Eriksson, B
Statistisk analys av nederbördsdata. Del II. Frekvensanalys av månadsnederbörd.
Norrköping 1980

Nr 18 Eriksson, B
Årsmedelvärden (1931-60) av nederbörd, avdunstning och avrinning.
Norrköping 1980

Nr 19 Omstedt, A
A sensitivity analysis of steady, free floating ice
Norrköping 1980.

Nr 20 Persson, C och Omstedt, G
En modell för beräkning av luftföroreningars spridning och deposition på mesoskala.
Norrköping 1980

Nr 21 Jansson, D
Studier av temperaturinversioner och vertikal vindskjuvning vid Sundsvall-Härnösands flgplats.
Norrköping 1980

Nr 22 Sahlberg, J and Törnevik, H
A study of large scale cooling in the Bay of Bothnia
Norrköping 1980.

Nr 23 Ericson, K and Hårsmar, P-O
Boundary layer measurements at Klockrike. Oct. 1977.
Norrköping 1980

Nr 24 Bringfelt, B
A comparison of forest evapotranspiration determined by some independent methods.
Norrköping 1980

Nr 25 Bodin, S and Fredriksson, U
Uncertainty in wind forecasting for wind power networks.
Norrköping 1980

Nr 26 Eriksson, B
Graddagsstatistik för Sverige.
Norrköping 1980

Nr 27 Eriksson, B
Statistisk analys av nederbördsdata. Del III. 200-åriga nederbördsserier.
Norrköping 1981

Nr 28 Eriksson, B
Den "potentiella" evapotranspirationen i Sverige.
Norrköping 1981

Nr 29 Pershagen, H
Maximisnödjup i Sverige (perioden 1905-70).
Norrköping 1981

Nr 30 Lönnqvist, O
Nederbördsstatistik med praktiska tillämpningar.
(Precipitation statistics with practical applications)
Norrköping 1981

Nr 31 Melgarejo, J W
Similarity theory and resistance laws for the atmospheric boundary layer.
Norrköping 1981

Nr 32 Liljas, E
Analys av moln och nederbörd genom automatisk klassning av AVHRR data.
Norrköping 1981

Nr 33 Ericson, K
Atmospheric Boundary layer Field Experiment in Sweden 1980, GOTEX II, part I.
Norrköping 1982

Nr 34 Schoeffler, P
Dissipation, dispersion and stability of numerical schemes for advection and diffusion.
Norrköping 1982

Nr 35 Undén, P
The Swedish Limited Area Model (LAM). Part A. Formulation.
Norrköping 1982

Nr 36 Bringfelt, B
A forest evapotranspiration model using synoptic data.
Norrköping 1982

Nr 37 Omstedt, G
Spridning av luftförorening från skorsten i konvektiva gränsskikt.
Norrköping 1982

Nr 38 Törnevik, H
An aerobiological model for operational forecasts of pollen concentration in theair.
Norrköping 1982

Nr 39 Eriksson, B
Data rörande Sveriges temperaturklimat.
Norrköping 1982

Nr 40 Omstedt, G
An operational air pollution model using routine meteorological data.
Norrköping 1984

Nr 41 Persson, C, and Funkquist, L
Local scale plume model for nitrogen oxides. Model description.
Norrköping 1984

Nr 42 Gollvik, S
Estimation of orographic precipitation by dynamical interpretation of synoptic model data.
Norrköping 1984

Nr 43 Lönnqvist, O
Congression - A fast regression technique with a great number of functions of all predictors.
Norrköping 1984

Nr 44 Laurin, S
Population exposure to So and NO_x from different sources in Stockholm.
Norrköping 1984

Nr 45 Svensson, J
Remote sensing of atmospheric temperature profiles by TIROS Operational Vertical Sounder.
Norrköping 1985

Nr 46 Eriksson, B
Nederbörds- och humiditetsklimat i Sverige under vegetationsperioden.
Norrköping 1986

Nr 47 Taesler, R
Köldperioden av olika längd och förekomst.
Norrköping 1986

Nr 48 Wu Zengmao
Numerical study of lake-land breeze over Lake Vättern, Sweden.
Norrköping 1986

Nr 49 Wu Zengmao
Numerical analysis of initialization procedure in a two-dimensional lake breeze model.
Norrköping 1986

Nr 50 Persson, C
Local scale plume model for nitrogen oxides. Verification.
Norrköping 1986

Nr 51 Melgarejo, J W
An analytical model of the boundary layer above sloping terrain with an application to observations in Antarctica.
Norrköping 1986

Nr 52 Bringfelt, B
Test of a forest evapotranspiration model.
Norrköping 1986

Nr 53 Josefsson, W
Solar ultraviolet radiation in Sweden.
Norrköping 1986

Nr 54 Dahlström, B
Determination of areal precipitation for the Baltic Sea.
Norrköping 1986

Nr 55 Persson, C (SMHI), Rodhe, H (MISU), De Geer, L-E (FOA)
The Chernobyl accident - A meteorological analysis of how radionucleides reached Sweden.
Norrköping 1986

Nr 56 Persson, C, Robertsson, L (SMHI), Grennfelt, P, Kindbom, K, Lövblad, G, och Svanberg, P-A (IVL)
Luftföroreningsepisoden över södra Sverige 2 - 4 februari 1987.
Norrköping 1987

Nr 57 Omstedt, G
An operational air pollution model.
Norrköping 1988

Nr 58 Alexandersson, H, Eriksson, B
Climate fluctuations in Sweden 1860 - 1987.
Norrköping 1989

Nr 59 Eriksson, B
Snödjupsförhållanden i Sverige - Säsongerna 1950/51 - 1979/80.
Norrköping 1989

Nr 60 Omstedt, G, Szegö, J
Människors exponering för luftföroreningar.
Norrköping 1990

Nr 61 Mueller, L, Robertson, L, Andersson, E, Gustafsson, N
Meso-γ scale objective analysis of near surface temperature, humidity and wind, and its application in air pollution modelling.
(Även serie Promis) Norrköping 1990

Nr 62 Andersson, T, Mattisson, I
A field test of thermometer screens.
Norrköping 1991

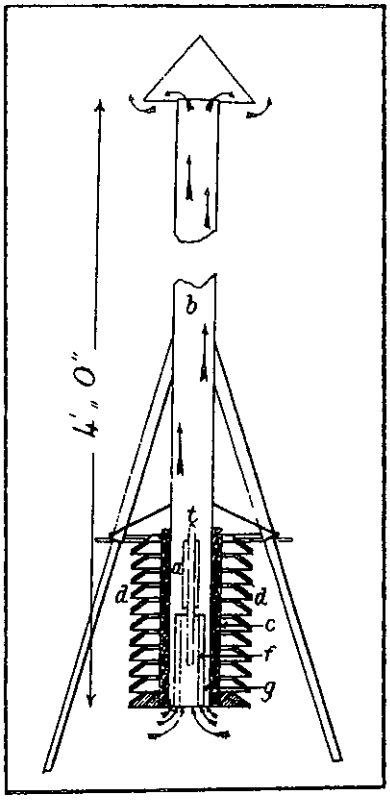

John Aitken, mostly known for his works in cloud physics, designed several screens. This one, from 1884, has a chimney to improve the ventilation.

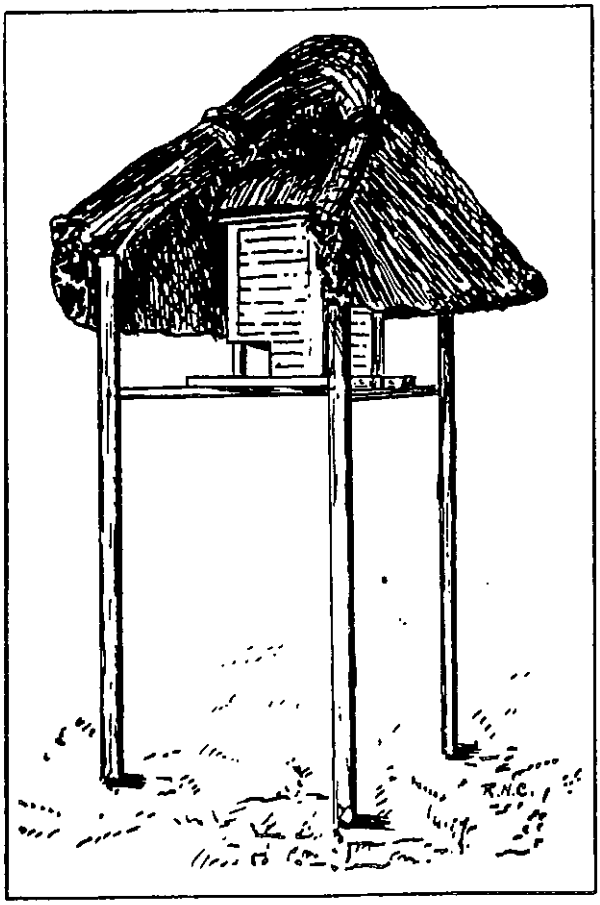

Wladimir Köppen, mostly known for his climate classification, advocated the Stevenson screen as an international standard. He also suggested some modifications, for instance a shelter above it for reducing the radiation error.

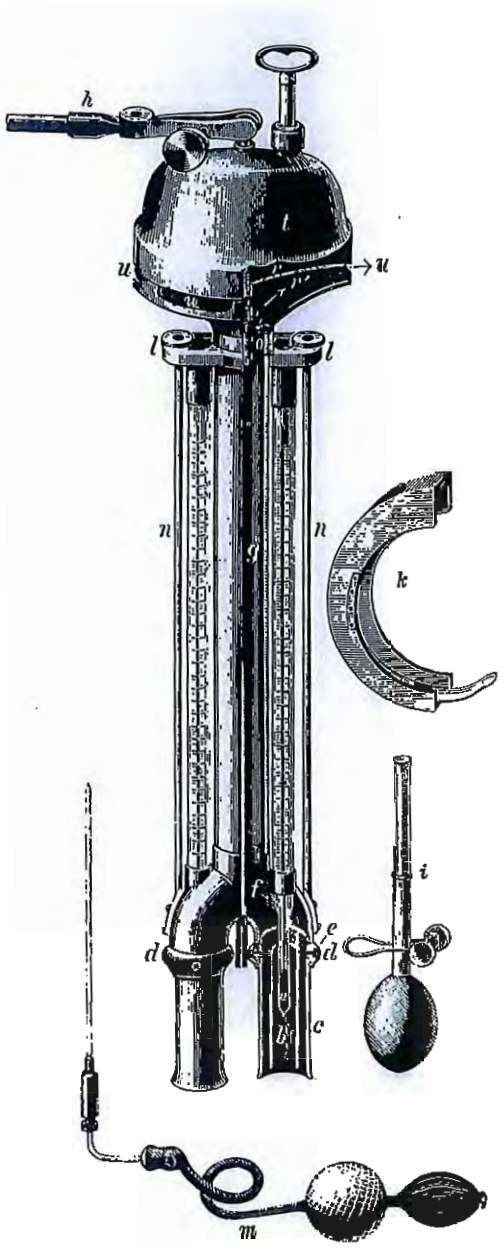

About 1890 Richard Assman designed an elaborate instrument for measuring the air temperature and humidity. It became known as the Assman psychrometer and considered a standard instrument. The Teledyne used here can be regarded as a development of this psychrometer.

SMHI
Swedish meteorological and hydrological institute
S-60176 Norrköping, Sweden. Tel. +46 11 15 80 00. Telex 64400 smhi s.

ISSN 0347-2116